HIGH THROUGHPUT EXPERIMENTATION:
A VALIDATION STUDY FOR USE IN CATALYST DEVELOPMENT

Submitted by

Niels Luchters

In fulfilment of the requirements for the degree of

Masters of Science in Engineering

University of Cape Town

May 2016

Synopsis

High throughput and combinatorial experimentation is becoming more and more used in catalysis research. The benefits of parallel experiments are not only limited to shorten the time-to-market, but also give opportunities to study the process in more depth by performing more experiments. The influence of a parameter, for example the amount of the active metal and/or promoter, to the process is better understood with a broader parameter space investigated.

To study the parameter space, multiple experiments need to be performed. It is of paramount importance to understand the variability of the data between these experiments. This is not always defined, specifically when literature gives contradictory results, most often due to the time for duplicate experiments necessary. In this project the reproducibility and variance in high throughput catalyst preparation and testing was determined and the use of parallel experimentation was demonstrated within a catalyst development study.

The high throughput equipment was used for catalyst development studies for fuel processing, the production of fuel cell-grade hydrogen from hydrocarbon fuels. Fuel processing consists of three catalytic reactions, namely reforming, water-gas shift and a CO clean-up through either selective methanation or preferential oxidation. Focus has been placed on the first two reactions, steam methane reforming (SMR) and medium temperature water-gas shift (WGS), using platinum group metals (PGM). All catalysts in this study (except for the commercial WGS catalyst) were prepared using automated synthesis robot (Chemspeed ISYNTH) and the activity testing was performed on the Avantium Flowrence.

For both reactions two types of studies were performed, one-to-many and many-to-many; referring to one catalyst tested in many reactors or many prepared catalysts (same composition, different batches) tested in many reactors. For the WGS one-to-many a commercial low temperature shift catalyst was selected and for SMR a single batch of Rh/Al_2O_3. The many-to-many experiments comprised of eight batches of prepared catalysts for both reactions. The WGS reaction was performed with 1 wt% Pt/Al_2O_3 catalysts and for the reforming reaction batches of 0.5 wt% Rh/Al_2O_3 was used. It was proven that in all these studies the experimental standard deviations in the data is 6%, from preparation to activity measurements.

A study on the rhodium metal loading on alumina in the steam methane reforming catalyst was studied between 0.05 and 0.6 wt%. A 0.4 wt% Rh/Al_2O_3 was found to have the highest activity per amount of rhodium. Lower Rh content would require decreased space velocity, whereas higher metal content does not increase the conversion due to larger crystals sizes. This study has been performed up to a metal loading of 0.6 wt% and it is recommended to follow-up with studying the range of 0.6 to ~2.5 wt% to investigate the optimal metal loading.

It was shown that the use of automated experimentation (parallel preparation and evaluation under same condition) for catalyst development results in highly reproducible results with a relative standard deviation of ~6% on the catalytic activity. The high throughput equipment was demonstrated to be a very powerful tool in catalyst research.

Acknowledgements

I would like to express my deepest gratitude to Prof. Jack Fletcher for giving me the opportunity to do this work in the field of high throughput experimentation and to complete my MSc on the topic. It was always a pleasure to discuss the fuel processing activities together. Your trust in me setting up and working with the state of the art equipment gave me the confidence to make this project successful. I would also like to thank Mr Stephen Roberts for his guidance and advice on the laboratory procedures and on the defining the setup. I am grateful to Mr Yi Zhou for his support in performing some of the experiments. Furthermore, I would like to give my thanks to all the support and technical staff of the Centre for Catalysis Research for keeping the laboratories running. Without them this project would not have been completed successful.

In addition, I am grateful for the support from HySA/Catalysis and the Department of Science and Technology for their financial contribution to this study.

Last but not least, I would like to thank my parents for their continuous support and encouragement.

Declaration

I know the meaning of plagiarism and declare that all the work in the document, save for that which is properly acknowledged, is my own

Signed by candidate

…… Date: 29 March 2016

Niels Luchters

Table of content

List of Figures

List of Tables

List of Equations

Nomenclature

Symbol	***Description***
%	Percent
Ag	Silver (element)
Al_2O_3	Alumina
Atm	Atmosphere (unit for pressure)
Au	Gold (element)
°C	Degrees Celsius
°C/min	Degrees Celsius per Minute
CH_4	Methane
CO	Carbon Monoxide
CO_2	Carbon Dioxide
Cu	Copper (element)
CuZnO	Copper Zinc Oxide
GC	Gas Chromatograph
GHSV	Gas Hourly Space Velocity (expressed at standard conditions, 0°C and 1 atm)
h	Hour
H_2	Hydrogen
H_2O	Water or steam
He	Helium (element)
HTE	High Throughput Experimentation (not to be confused with the company hte GmbH)
HTS	High Temperature Shift
IC	Internal Combustion
ICP-OES	Inductive Coupled Plasma – Optical Emission Spectrometer
IWI	Incipient Wetness Impregnation
kJ mol^{-1}	Kilo Joule per Mole
LTS	Low Temperature Shift
m^2/g	Square meter per gram
MFC	Mass Flow Controller
min	Minutes
N_2	Nitrogen
Ni	Nickel
nm	nanometer
PIC	Pressure Indicator Controller
P&ID	Piping and Instrument Diagram

PGM	Platinum Group Metal
PPQ	Pora Plot Q
Pt	Platinum (element)
Rh	Rhodium
RSD	Relative Standard Deviation
SA	Surface Area
S/C	Steam to Carbon Ratio
SiC	Silica Carbide
SGHSV	Standard Gas Hourly Space Velocity (see GHSV)
Sml/min/reactor	Standard millilitres per minute per reactor
SMR	Steam Methane Reforming
SS	Stainless Steel
TCD	Thermal Conductivity Detector
ToS	Time on Stream
µl/g	Microliter per gram
µl/min	Microliter per minute
Vol%	Volume percent
WGS	Water-Gas Shift
wt%	Weigh percent
Zn	Zinc (element)

1 Introduction

The world's energy demand has been increasing exponentially over the past hundred years with the increase in population globally. Fossil fuel, about 85% (Acar & Dincer, 2015:1757), plays a very important role in generating this energy. With more governments planning to implement a 'carbon tax' on the production of CO_2, makes the use of alternative energy sources more attractive. However, no single technology for replacing oil based society exists. Alternative energy sources all have their own benefits and challenges for various applications in the current society (economic, environmental and social impact).

Hydrogen is the fuel of choice for most type of stationary and mobile fuel cells and is a promising technology for generating electricity with high fuel efficiency. This technology is getting more attention as the developments progresses rapidly and changing of governmental regulations towards emissions. Fuel cells bring solutions as a power source for vehicles as well as back-up power and grid electricity generation. Specifically, fuel cells have the potential to supply electricity with high efficiency in remote locations where the capital costs to extend the national grid are too high. However, the lack of a proper hydrogen infrastructure (production, storage, distribution) will not see the implementation of fuel cells.

Hydrogen is one of the most abundant elements in the universe, although not sourced as a natural occurring resource and a process is required to 'extract' hydrogen. Natural resources from which hydrogen can be 'extracted' include water, fossil fuels and biomass. It is anticipated that in the long term future hydrogen is generated using carbon-free technology from renewable resources, such as solar PV and electrolysers, but current technology remains too expensive and efficiency needs to be improved (Acar & Dincer, 2015:1763). In a transition period (near and middle term future) to a carbon-free renewable hydrogen economy, fossil fuel reforming should be considered as an efficient method using widely available fuels (Dincer & Zamfirescu, 2012:16266).

Fuel processing is an attractive technology to convert fossil fuels (like natural gas, LPG (liquefied propane gas), diesel, jet fuels, etc.) into hydrogen or syngas. Utilising the globally existing infrastructure for these fuels, hydrogen can be produced on side and, after clean-up, directly used in fuel cells or stored.

In catalyst development, traditionally, a single catalyst is prepared and tested for performance. However, the use of parallel experimentation, called high throughput experimentation, for the discovery, development and optimisation is getting increasing acceptance (Maier, Stöwe & Sieg, 2007:6017). Over the years more state-of-the-art technologies for catalyst research have been developed, including catalyst preparation, catalyst testing and data handling software.

2 Background and literature review

As globally more emphasis is put on non-fossil fuel derived energy, the hydrogen economy will become more important. Hydrogen is considered to be the most interesting energy source, as it has a high energy density (by weight; Figure 2-1) and its abundance is (potentially) endless. However, hydrogen remains stored inside other molecules and needs to be “extracted”. One such method to obtain hydrogen is to reform hydrocarbon feedstock.

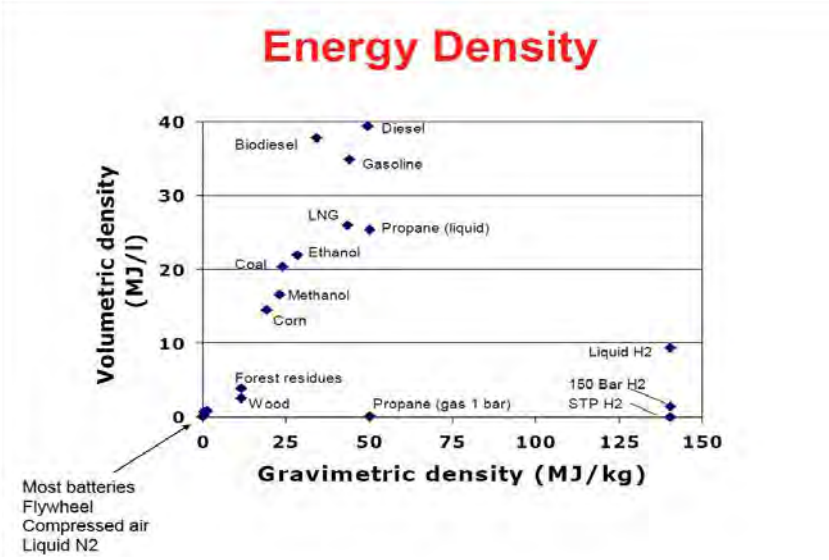

Figure 2-1: Comparison of energy densities of various fuels; (available: http://www.olicognography.org/graph/energydensity.jpg)

Fuel cell is a technology to generate electricity from hydrogen. Even though the efficiency of internal combustion (IC) engines are performing better over time, the efficiency of fuel cells are typically higher (Figure 2-2). Where IC engines have an overall efficiency of about 20% (energy produced from the total energy of the fuel), fuel cells can reach efficiencies of twice that. However, fuel cells require hydrogen as a fuel and, even though hydrogen has a high gravimetric density, it has a very low volumetric density. For vehicles this low volumetric density is overcome by using 300 bar, or even 700 bar, cylinders, but it becomes a problem when the application is placed in remote areas. Preferably non-explosive liquid fuels with existing infrastructure are required for the technology to be implemented in remote areas (off-grid), until such a time sufficient renewable hydrogen infrastructure is in place. Diesel and LPG are widely available hydrogen carriers. Fuel processing is the method to convert the hydrocarbon fuel into hydrogen suitable for fuel cells.

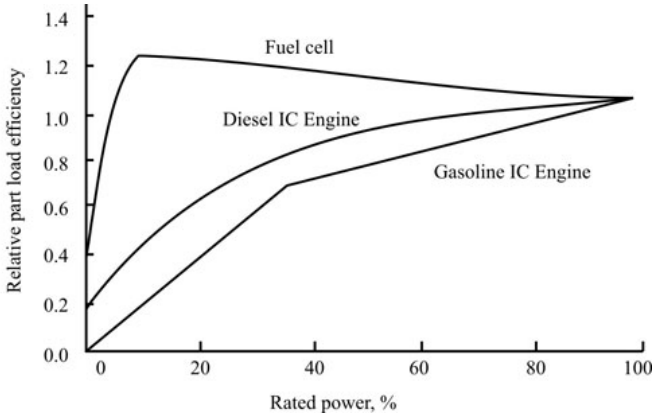

Figure 2-2: Relative load efficiencies of fuel cells versus internal combustion engines; (available: http://nptel.ac.in/courses/112104033/lecture35/35_6.htm)

PEM fuel cells

Polymer electrolyte membrane (PEM) fuel cells, also called proton exchange membrane, are a promising technology for highly efficient and clean power generation. They are ideal for stationary and mobile applications, like remote electricity generators and vehicle power source, and are considered twice as efficient as the internal combustion engine (Farrauto et al., 2003:1). PEM fuel cells work on the principle of converting chemical energy into electrical energy. Hydrogen is fed to the fuel cell on the anode side, where a platinum catalyst splits it into hydrogen ions (protons) and electrons. The polymer electrolyte membrane allows only the positively charged protons to pass to the cathode side of the fuel cell. The negatively charged electrons must travel through an external circuit to the cathode, generating an electrical current. At the cathode side the protons and electrons are reacted with oxygen (often from air) to form water (U.S. Department of Energy [USDOE], n.d.). A schematic drawing of a single cell PEM fuel cell is given in Figure 2-3. A typical fuel cell system is composed of multiple stacked cells to generate more power.

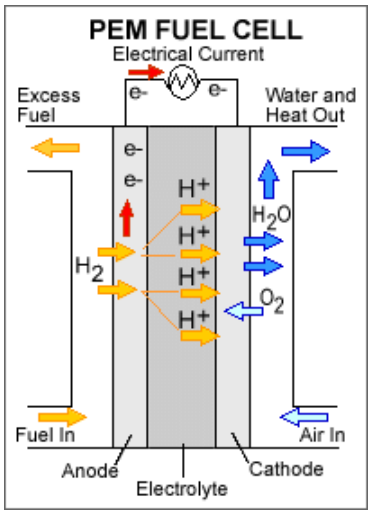

Figure 2-3: Polymer electrolyte membrane fuel cell (Energy.gov, n.d.).

Hydrogen production via fuel processing

The fuel processing of low-cost fossil fuels through reforming can provide the commercial hydrogen production capacity required to establish the hydrogen infrastructure in the near future. Even when renewable low-carbon energy resources are implemented, fuel processing is expected to augment the hydrogen supply. Currently, renewable technologies are not matured enough to rely 24/7 on their electricity generation with current living standards (energy dependencies).

Hydrogen can be reformed via partial oxidation, autothermal reforming or steam reforming, the latter being most widely used process for hydrogen production from natural gas. Steam reforming of natural gas, containing mostly methane, at large industrial scale is a mature production process operating at high temperatures (above 700°C) in the presence of a supported nickel catalyst. However, the technology for small scale fuel processing for fuel cells (~1-10kW) still needs to be developed.

Steam reforming of fossil fuels, like methane (CH_4), produces a hydrogen rich mixture called reformate, but also carbon monoxide (CO). CO is considered a poison for PEM fuel cells as the CO adsorbs on the platinum active sites and deactivates the fuel cell catalyst. For low temperature PEM fuel cells the maximum CO concentration in the reformate is ~10 ppmv and, typically, after reforming the CO content in the effluent is approximately 10 vol%. Thus further CO clean-up is required before use by a fuel cell. A secondary reaction to this reaction is the water-gas shift (WGS) reaction, converting CO into CO_2. Often, the WGS reaction occurs in the reforming reactor, however, WGS reaction requires a low temperature to drive the CO conversion further. The second reactor stage in the fuel processor is the WGS reactor operating at a much lower temperature (200-400°C). Depending on the process conditions (temperature and gas composition) the CO concentration is brought down to ~1 vol%. Further clean-up of the CO is done through either selective methanation, where the relative low quantity of CO is converted back to CH_4, or preferential oxidation in which the CO reacts with oxygen (from added air) to CO_2.

2.1 Steam methane reforming

Through steam reforming hydrogen is produced from the methane as well as from the steam. For every methane reformed to CO_2 (including the WGS step), 4 H_2 are produced. Although, longer hydrocarbons (HC_{2+}) are easier to reforms, from all reforming technologies and available feeds methane steam reforming (SMR) produces most hydrogen per CO_2 formed. However, SMR is strongly endothermic and thus requires a lot of heat.

Steam reforming is the conversion of hydrocarbons into CO and H_2 (Reaction 1) by using steam, however, the reformate often contains significant amounts of CO_2. The latter is formed by the consecutive water-gas shift reaction (Reaction 2) occurring partly in the reformer.

$CH_4 + H_2O \rightarrow CO + 3H_2$ $\quad \Delta H°_{298} = 206.2 \text{ kJ mol}^{-1}$ **Reaction 1**

$CO + H_2O \rightarrow CO_2 + H_2$ $\quad \Delta H°_{298} = -41.2 \text{ kJ mol}^{-1}$ **Reaction 2**

The steam reforming reaction is an equilibrium reaction, dependant on temperature, pressure and steam to carbon ratio (S/C) (Figure 2-4). Although, industrially the

steam reforming is performed at high pressures, because of the requirements for downstream processes (Kolb, 2008:19), the equilibrium conversion is increased at low pressures. In order to obtain nearly full conversion of the methane the reaction temperature should be above 700°C, atmospheric pressure (which is for commercial purposes a safety requirement) and a S/C ratio of 3 or more.

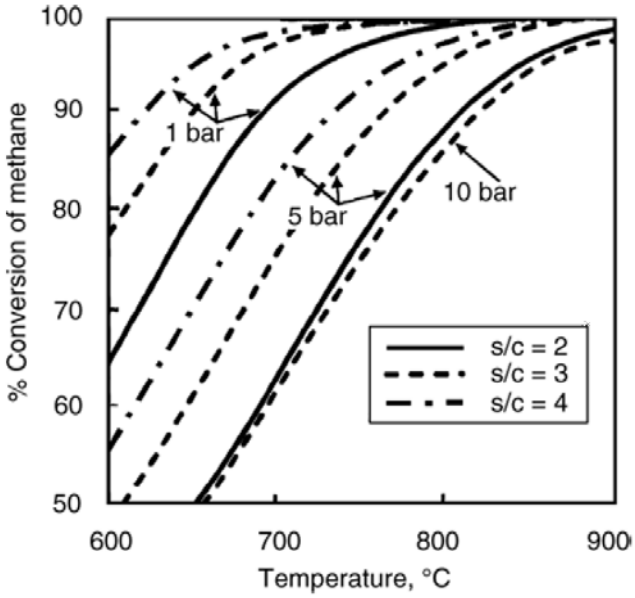

Figure 2-4: Equilibrium conversion for steam methane reforming reaction (Joensen and Rostrup-Nielsen, 2002)

The need for platinum group metals

All the conversion stages of the fuel processor are catalytic although, in cases where the feed contains sulphur, the desulphurization step may employ a sorbent. Whereas well established catalysts exist for almost all the catalytic stages (as typically employed in industrial hydrogen and syngas plants), these base-metal catalysts are in need of lengthy and delicate activation (reduction) procedures and remain susceptible to re-oxidation by oxygen ingress (Farrauto et al., 2003:1). It is therefore generally anticipated that, for portable and standby fuel cell applications, fuel processor catalysts will be formulated from platinum group metals, both for reason of the nobility (stability with respect to oxidation) and their high activity versus base-metal catalysts. The latter essential for the development of the small fuel processing foot print desired for small (1 – 10 kW) power modules.

In the case of methane steam reforming, the industrially used Ni catalysts are cost effective, but have a number of additional drawbacks ontop of those mentioned above. The Ni catalyst are highly susceptible towards coke formation and thus require careful reaction control, they are vulnerable to sulphur poisoning, and highly pyrophoric when exposed to oxygen. Precious metals in the platinum group can overcome some of these issues and have a higher activity than Ni as well (Kolb, 2008:80).

Catalysts

Over the last three decades many publications have been reported on platinum group metal (PGM) supported catalysts for steam methane reforming. A study on PGM reforming activity was published by Rostrup-Nielsen (1973). The active metals were supported on alumina and magnesia and were ranked according to activity:

Rh, Ru > Ni, Pd, Pt > Re > Co

Rostrup-Nielsen (1984:66) has reported the ranking of PGM based on turnover numbers. For methane steam reforming using silica-supported catalysts they found:

Rh (1.6) > Ru (1.4) > Ni (1) > Pd (0.6) > Pt (0.5)

Whereas for ethane steam reforming using alumina supported catalysts:

Rh (13) > Ru (9.5) > Pd (1.0) ~ Ni (1.0) > Pt (0.9)

This shows that it is evident that rhodium is the more interesting metal, being one order of magnitude more active than nickel or platinum. Although, rhodium catalysts are extremely costly they give the possibility for downscaling the size of reactors.

Properties of the support are known to play an important role in catalytic reactions. For instance, a high active surface area results in better dispersion of the active metal and good porosity will increase contact-time between the reactants and the catalyst. But also the chemical bonding interactions between the support and the metal will have an effect on the activity and stability (Wang, 1998).

Alumina is widely used as support material for high temperature steam reforming but many groups also report on rare earth oxides, such as ceria, zirconia or mixtures thereof (Trimm and Önsan, 2001). These show high activities, due to their oxygen storage capacity, however, long term stability data for high temperature steam reforming is often not shown. Ligthart, Van Santen & Hensen (2011) have investigated the influence of particle size on the activity for supported rhodium catalysts on ceria, zirconia, silica and mixtures thereof. They found that the intrinsic rate per surface metal atom increases linearly with the dispersion independently of the support. Rhodium particles smaller than 2.5 nm deactivate more strongly due to the oxidation of the very small particles under steam methane reforming conditions.

2.2 Water-gas shift

Water-gas shift (WGS) reaction has a thermodynamic equilibrium and is mildly exothermic (Reaction 2). The WGS reaction typically occurs also in the reformer reactor as a subsequent reaction once CO has been formed and high quantities of steam (S/CO) are present. However, the high temperature of the reformer limits the equilibrium conversions of CO. Typically, in a reformer operating at 700°C and S/C of 3-4, a CO conversion of 50% is observed (approx. 8vol%). A lower temperature WGS reactor is required before selective methanation or preferential oxidation can reduce the CO to > 10 ppmv.

$$CO + H_2O \rightarrow CO_2 + H_2 \qquad \Delta H^\circ_{298} = -41.2 \text{ kJ mol}^{-1}$$ **Reaction 2**

In industrial two WGS reactors are used to lower the CO concentration with producing some additional H_2. A first reactor containing chromium oxide stabilised iron oxide catalyst is operated at high temperature (350 - 450°C) to reach equilibrium, called high temperature shift (HTS). Due to the exothermic reaction and

high conversions of CO during the HTS, the reactor temperature increases along the catalyst bed (adiabatic) (Kolb, 2008).

Subsequent to the HTS is a low temperature shift (LTS) reactor using a copper/zinc oxide catalyst. The LTS catalyst is highly sensitive to sintering requiring stringent controlled temperatures (~195-220°C) and slow reductions, but typically less CO has to be converted in this stage (much lower temperature increase in the reactor). For example, a runaway reaction, due to its exothermicity, will increase the temperature and deactivate the LTS catalyst.

In portable fuel processing devices, the CuZnO catalyst is not suitable and a single HTS stage would not convert enough CO for further clean-up (preferential oxidation or selective methanation; not part of this project). Platinum group metals are active for WGS but typically are less active then CuZnO. The temperature range for PGM catalysts are 275 - 350°C with shorter lifetimes. Catalyst optimisation studies for PGM formulations are focussed on activity increase at low temperature (to improve lifetime and higher conversion).

2.3 High throughput methodology and equipment

The terms of "high throughput experimentation" and "combinatorial screening" are often interchangeably applied (Potyrailo et al, 2011:580). Even the IUPAC defined high throughput screening as the "process for rapid assessment of the activity of samples from a combinatorial library or other compound collection, often by running parallel assays in plates of 96 or more wells" (Maclean et al, 1999:2354). In the late nineties combinatorial chemistry was mainly used in pharmaceutical research and the term was applied specifically to that field. Maier, Stöwe & Sieg redefined the terms for the material sciences and chemical industry[1], such that the term refers to a change in the nature of the parameters, not to change the value of the parameter. The systematic change of parameters, like composition, temperature, pressures, etc., to explore a wide parameter space is defined as high throughput experiments (Maier, Stöwe & Sieg, 2007:6017). High throughput experimentation also makes use of parallelization: performing multiple experiments in parallel under similar conditions with variation in the studied parameter. In this thesis high throughput experimentation is referred to parallel experiments.

High throughput experimentation has been applied to science since the early twentieth century by Edison in 1878, Ciamician in 1912, and the development of the catalyst for ammonia synthesis by Mitasch at BASF in 1909 (Maier, Stöwe & Stieg, 2007). Despite this long history only in the late 1990s did the methodology commercialize, partly favoured by the technology-friendly venture capital boom. Commercial enterprises focusing specifically on high throughput experimentation such as SYMYX, Chemspeed, hte GmbH, and Avantium found their way to the market. Although in research much scepticism still exists for the method, more acceptance is seen for the use of the technology, specifically with large industrial companies.

High throughput experimentation (HTE) is a very valuable tool for research into catalyst development as well as process optimisation. With performing the experiments in parallel, and often continuous on-line analysis, more data can be

[1] "The term 'Combinatorial' should refer to experiments in which groups or elements of different materials or components of a recipe, such as solvents, additives, or other components, are combined." (Maier, Stöwe & Sieg, 2007)

generated as well as the reproducibility of the data is increased. Combining large data sets of on-line analysis with the process parameters for multiple reactors requires automation of the equipment, and when not done properly data can be lost or misinterpreted. More important is the huge advantage automation gives to reproducibility of experiments. When executing a specific defined recipe (programmed), all other times the same programme is repeated same results should be obtained. Reproducibility of experiments is of extreme importance to the research but is rarely being proven due to the time constraints.

The large amounts of data generated through HTE calls for adequate date workup. Such workup involves combining the analytical data with the process data for each particular experiment. These workup proceedings are ideally performed through a database to keep consistency in the data.

Automation and the data workup through databases make the HTE technology costly. However, the reduction of potential research time ('time-to-market') makes the technology very interesting. For example, data for patents or publications can be generated in shorter time and can give you an advantage over competitors. Also, it can open up the possibility to generate more knowledge on a reaction or mechanism within less time, e.g. parallel lifetime studies for poisoning or multiple conditions.

SYMYX

Symyx Technologies was founded in 1994 and were one of the leaders in the high throughput experimentation development. However, in 2010 their laboratory robotics technology spun out as the company Freeslate, Inc. and the remaining business was merged with Accelrys, now being Biovia. Freeslate is currently part of Unchained Labs and have state-of-the-art robotics technology for high throughput research. Although, Symyx addopted the pharmaceutical high throughput principles into the chemical industry for catalysis research, Freeslate's mission statement currently is "to accelerate drug development through powerful automation" (Freeslate, 2016).

hte GmbH

hte GmbH was founded in 1999 in Germany and is owned by BASF SE. This match with BASF gave hte GmbH their focus for the chemical industry. The company is one of the leaders in providing technology and services for enhancing research and development. Their main areas are in chemical, energy, refining, environmental and materials industries (hte-company, 2016).

Throughout the years, hte GmbH has developed various high throughput reactors. The equipment ranges from the parallel reactor setups to 'sub-pilot' scale reactors for large scale lab testing. Each reactor in the parallel setup is controlled independently, and thus the lab space footprint remains relatively large.

Avantium

Avantium was founded in 2000 following a spin-out from Royal Dutch Shell. In the early years, Avantium had a very broad portfolio of services on offer, from research services for chemical industry to pharmaceutical synthesis and crystallisation screening. Today, their offerings include catalytic research and development and providing complete high throughput technology systems, specifically for the chemical industry. Next to these, Avantium has a number of its own internal development programmes to commercialise products for renewable chemistries (Avantium, 2016).

One of the systems they provide to customers is the Flowrence, a 16 parallel fixed-bed reactor setup customised to the customer's chemical process. The Flowrence high throughput system is fully automated with running programmable recipes and integrated on-line analytics.

Chemspeed

Dr. Rolf Gueller founded in 1997 the company Chemspeed Technologies AG in Switzerland. Chemspeed is a provider of high throughput, or what they rather call 'high output', platforms (Chemspeed, 2015).

Although, from the start Chemspeed focussed more on the pharmaceutical industry, as well as cosmetics, food, material science and home care, rather than the chemical industry. The technologies they have on offer are tailored for synthesis type work (batch type reactors) and this is ideal for catalyst preparation.

All their equipment is software controlled and mostly consists of a platform with various tools, like dispensing, weighing, sonication, barcode reading, etc. These modular tools make the platform flexible and easily customisable to the required synthesis procedure. More on the Chemspeed platform as used in this project in section 4.1.1, including description of the tools.

Integrated Lab Solutions GmbH

ILS (Integrated Lab Solutions GmbH) is a private company based in Germany and was founded in 2005. ILS focusses on providing services (simulation, design, and testing) as well as equipment. The high throughput equipment they offer is customised for chemical processes with various parallel reactor type platforms available (ILS, 2016).

2.4 High throughput catalyst development

One of the examples of using high throughput tools in fuel processing catalyst development is from a collaboration between Symyx and Honda Motor Company. In 2007, researchers from Honda reported results of a combinatorial catalysis study of over 250 000 materials. They claimed that catalysts containing a combination of a) one noble metal like Pt or Rh, b) one group 11 metal like Cu, Ag or Au, and c) one partially reducible oxide like ceria, zirconia, titania, lanthana, vanadia or mixed metal oxides thereof, form improved WGS activity in the low–medium temperature shift range (Hagemeyer et al., 2007).

These large amount of formulation screenings were performed in Symyx equipment and measured on-line for activity. The catalyst materials were prepared with a synthesis robot in small quantities and placed on a wafer structure of approximately 3 inch. They deposited about 100 different catalyst formulations on each wafer. Before the catalyst screening the wafers were calcined and/or reduced. Subsequently, the wafers were placed in a holder with XY movement. Heat was provided from the rear of the wafer to each catalyst material independently using a CO_2 laser. A scanning mass spectrometer with a 'sniffing' probe measured gas compositions at each catalyst on the wafer (Hagemeyer et al., 2004). This method of high throughput experimentation, allowed for screening of large numbers of materials in short times and rank them according to CO conversion and CO_2 formation.

Morra et al (2007: 380) presented a kinetic study of *o*-xylene hydrogenation and characterisation of oxygen storage capacity of ceria-doped catalysts. The high throughput equipment used for this study was a SWITCH 16 reactor system developed by AMTEC GmbH and IRC-CNRS within the frame of a joint EU programme. The reactor setup was composed of two 16 port valves, upstream and downstream of the 16 reactors, to select a single reactor that will see feed gas and is analysed, while all others are placed under an inert gas. Such setup is ideal for fast and short experiments, however, does not lent itself for the longer lifetime studies as it is not a parallel screening setup.

3 Aim and objectives of the study

The overall aim of this work was to demonstrate high throughput experimentation as a tool for catalysis research and development. A set of objectives were established to demonstrate the aim. The following objectives were studied:

- The first objective was to prove the reproducibility of catalyst preparation by incipient wetness impregnation. Series of catalysts were prepared in parallel and characterised (using conventional techniques) for active metal loading and crystal size.
- To assess and validate the reproducibility of the high throughput testing equipment through analysing catalytic performance in parallel reactors. The study was performed on two case studies: medium temperature water-gas shift and high temperature steam reforming.
- The third objective was to determine the influence of metal quantity at low loadings using high throughput techniques.

4 Experimental

In this project two state-of-the-art equipment were used. Both equipment make use of the principle of high throughput experimentation through parallelisation under similar condition. For the catalyst preparation the Chemspeed ISYNTH was used and the catalyst testing was performed on the Avantium Flowrence. The validation performed in this study involved both equipment for two case studies, water-gas shift and steam methane reforming reaction, all under fuel processing conditions.

4.1 Catalyst preparation

Various catalysts were prepared for water-gas shift and steam methane reforming. All catalysts, with the exception of a commercial low temperature shift catalyst, contained platinum group metals and will be used in fuel processing (the production of hydrogen for fuel cells). The catalysts were prepared using the Chemspeed ISYNTH, a synthesis robotic arm. For comparison one similar catalyst was prepared by hand using conventional glassware, mimicking all the steps of the automated Chemspeed preparation method.

4.1.1 Chemspeed equipment and setup

The Chemspeed ISYNTH (further referred to as Chemspeed) platform is designed for chemical synthesis and reactions. The Chemspeed (Figure 4-1) consists of a robotic arm, various tools and parallel reactors vessels (the layout of the platform is shown in Appendix 9). The robotic arm can pick up any of the tools to perform tasks (e.g. volumetric or gravimetric aspiration and dispensing, sonication). The tools that the arm can pick up include volumetric dispenser, gravimetric (viscous) liquid dispenser, gravimetric powder dispenser, sonication probe, barcode reader, (de-)capper (to cap reactor vessels) and a gripper (to move reactor vessels). To prepare the catalysts for this project the volumetric dispenser and gravimetric powder dispenser (Figure 4-2) were used. The powder dispenser was used to weigh the support material (Al_2O_3) in each reactor vessel. The volumetric dispenser was used to dilute the metal solutions and perform the impregnations. The metal salts were weighed by hand due to the costs of the salts and their ‘stickiness’ (hydroscopic salts).

Figure 4-1: Photo of the Chemspeed ISYNTH; (available: http://www.chemspeed.com/synthesis/isynth-3/).

Figure 4-2: Chemspeed tools used to prepare catalysts; Left volumetric dispenser (four needle tool), right gravimetric powder dispensing.

The ISYNTH reactor vessels used are 40 mL size and 24 reactor vessels can be used in parallel at a time. The reactor block with the 24 reactor vessels (Figure 4-3), contains a heating zone, reflux plate and top plate for evaporation. The reactor vessels are located in the heating zone with a reflux zone in the top. The reactor block contains an orbital shaker for mixing. The liquid and powder dispensing tools both can dispense into each reactor vessel and, in the case of the liquid dispensing, dispensing while shaking.

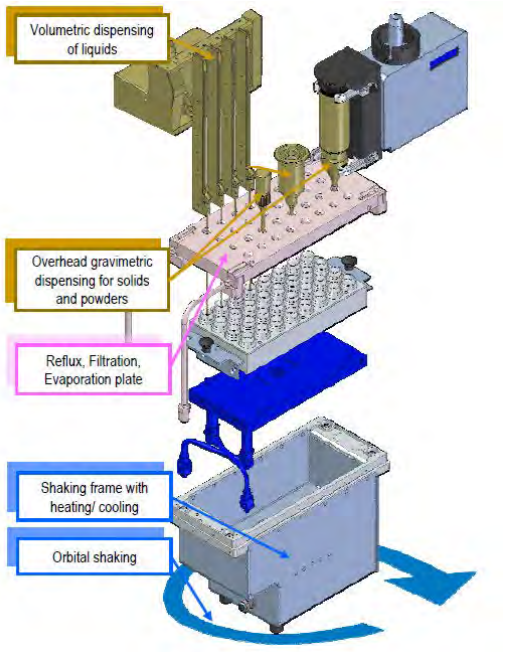

Figure 4-3: ISYNTH reactor block composition; (available: http://www.chemspeed.com/synthesis/isynth-3/).

The Chemspeed is able to execute tasks programmed in the software. A series of tasks, forming the recipe, can be executed multiple times and a standard recipe was made for preparation of all catalysts used in this project. Refer to section 4.1.3 for details on the preparation methods.

4.1.2 Incipient wetness impregnation

To prepare the catalysts in this project a standard method was used. Except for the commercial catalyst (LTS), all catalysts were prepared by incipient wetness impregnation (IWI) using the Chemspeed ISYNTH synthesis robot (more details on the method for high throughput preparations below (section 4.1.3).

The Pt/Al_2O_3 and Rh/Al_2O_3 were prepared using Sasol-Alumina's Puralox alumina NWA-155. Stock solutions of chloroplatinic acid and rhodium nitrate (Sigma-Aldrich) of sufficient concentration, so as to ultimately prepare catalyst with desired metal loading, were prepared by weighing appropriate amounts of metal salts and dissolved in de-ionised water in a volumetric flask to obtain the correct concentration. These stock solutions were used by the Chemspeed ISYNTH robot to prepare diluted impregnation solutions of appropriate concentration for impregnation. The catalysts were prepared by adding 1.4 mL of appropriately diluted impregnation solution with PGM salt to 2 g of accurately weighed support via a fine injection needle, whilst under continual shaking. Thereafter, the catalysts were evacuated to 500 mbar and dried at 30°C for 1 hour under continuous vigorous shaking to ensure good mixing and contact between support and impregnation solution. The catalysts were dried at atmospheric pressures and 60°C for 2 hours, and further drying at 120°C for 4 hours. Subsequently, catalysts were calcined at 500°C for 5 hours (for WGS catalysts) or 800°C for 5 hours (for reforming catalysts) in air by ramping the temperature 1°C/min.

4.1.3 High throughput impregnations

The catalysts for the high throughput studies were prepared by incipient wetness impregnation on the Chemspeed ISYNTH. A single recipe was made for all batches of catalysts. Except for preparing metal salt stock solutions and calcination of the catalysts, all steps described above were performed by the Chemspeed robot.

From the PGM stock solutions the Chemspeed transferred required amounts to a series of vials and added de-ionised water to obtain sufficient concentration of the PGM salt for impregnation in 1.5 ml. For mixed metal co-impregnations (not part of this project) multiple metal salt solutions can be combined to form a series of multi-metal impregnation solutions (variations in metal concentrations can easily be made to vary the metal ratios of the catalysts). 1.4 mL of each impregnation solution was added to 2 g support material and (minimum) 100 µL of the impregnation solution cannot be used, as the needle of the Chemspeed robot is not able to aspirate this. The 100 µL should be considered waste. A maximum of 24 catalysts can be prepared in parallel at a time with the Chemspeed using this method.

4.2 Catalyst characterisation

To determine the reproducibility of the high throughput equipment, many catalyst batches were prepared for this study. Due to the long analysis duration of the catalyst characterisation equipment (low throughput), only limited characterisations were performed. The analysis focussed on in this study are those that support the study objectives.

CO chemisorption

CO chemisorption was performed on the 1 wt% Pt/Al_2O_3 catalyst series in a Micromeritics ASAP 2000 equipped with two Edwards vacuum pumps (E2M-0.7).

The powdered sample was heated to 250°C with a ramp rate of 5°C/min in flowing H_2 to remove adsorbed water and reduce the Pt metal. The sample was maintained at 250°C for one hour, after which the H_2 flow was stopped and the sample chamber was evacuated to a pressure of 1 µm Hg for two hours. The temperature was subsequently lowered to room temperature with 5°C/min, at which CO chemisorption was performed. It should be noted that the chemisorption results are calculated based on the nominal metal loading of 1 wt% (not related to the ICP results as potential errors from ICP will result in erroneous data).

ICP analysis

A Varian 730 ICP-OES (inductively coupled plasma - optical emission spectrometer) instrument was used to determine the metal content of fresh (unused) catalysts. The sample was digested with a mixture of hydrochloric, hydrofluoric and nitric acids in a MARS-5 microwave digester, followed by neutralization with boric acid prior to analysis.

4.3 Catalyst performance screening

The catalytic performance was evaluated using the high throughput equipment Flowrence from Avantium Technologies (referred to as Flowrence; Figure 4-4). The Flowrence consists of mass flow controllers and liquid pumps to make up the feed, 16 parallel fixed bed reactors, a selector valve and effluent analyser. The Flowrence is customised for water-gas shift and high temperature steam reforming reactions. The conditions are programmable via its software.

Figure 4-4: Photo of Avantium's Flowrence 16 parallel fixed bed reactor platform. (Avantium, 2016)

4.3.1 Flowrence equipment and setup

The Flowrence equipment consists of three sections: 1) Upstream including the gas and liquid feed mixing and flow distribution; 2) the reactor section with 16 parallel fixed bed reactors; and 3) downstream comprising the parallel pressure regulators, selector valve and on-line analysis. Refer to Appendix 9.2 for a detailed P&ID (piping and instrument diagram).

Upstream section

The upstream section of the Flowrence consists of 7 mass flow controllers (MFC), namely methane, nitrogen, hydrogen, carbon monoxide, carbon dioxide, air (not used in this project) and helium, and one liquid high pressure pump for water. The MFCs make up the feed gas composition and mixed through diffusion in the tubing (no static mixture). The dry gas mixture and the water feed are combined as a wet stream in the reactor before reaching the catalyst bed. The dry gas and liquid feed each have its own flow distribution.

The flow distribution is based on an equal pressure drop to each reactor. The pressure drop is created by passing the gas or liquid through a narrow capillary causing a resistance. By calibrating the resistance to each reactor an equal flow distribution is obtained. Each reactor has a capillary from the dry gas feed and a capillary for the water feed (Figure 4-5). In total there are 16 dry gas capillaries (ID 50 µm, 100 cm) and 16 liquid capillaries (ID 50 µm,175 cm).

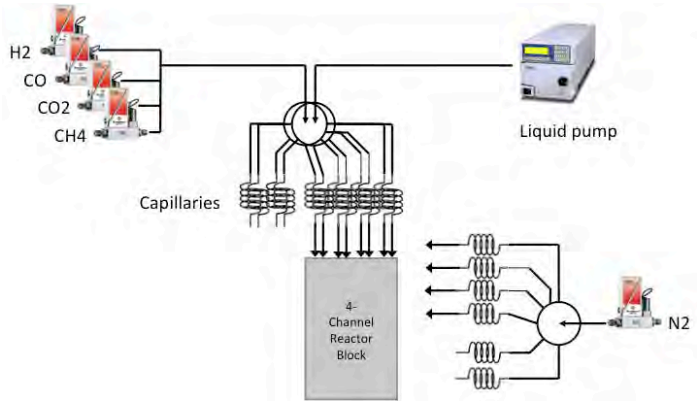

Figure 4-5: Schematic drawing of the distribution of dry gas and liquid to each reactor using pressure drop over capillaries.

Reactor section

The reaction section is comprised of 4 heating blocks, each containing 4 reactors, summing up to 16 parallel reactors. The reactors are a fixed bed setup and these reactor tubes are made of stainless steel (SS) or quartz, depending on the temperature and chemistry.

Both, the dry gas and water feed capillaries are mixed at the top of the reactor tube (upstream of the catalyst) where the water is evaporated and mixed with the dry gas. To improve the evaporation of the water and reduce flashing of droplets, the top of the reactor contained silica carbide (SiC). The catalyst is loaded in the reactor tube at such a length that it is placed in the isothermal zone of the heating block. Directly below the catalyst bed (downstream) is a plug of quartz wool and SiC to assist in positioning the catalyst bed in the reactor tube. An SS or quartz frit (porous filter) is placed at the bottom of the reactor tube to keep all the content in the reactor tube.

The reactor tube is placed in the heating block with a Viton o-ring at the top of the reactor, so that the reactor tube ‘hangs’ in the reactor block (see Figure 4-6 for a cross-section of the reactor setup). The lid, closing airtight on the o-ring, closes the top of the reactor. The o-ring is not placed directly onto the heating block, but instead on an actively cooled plate to protect the o-ring from melting.

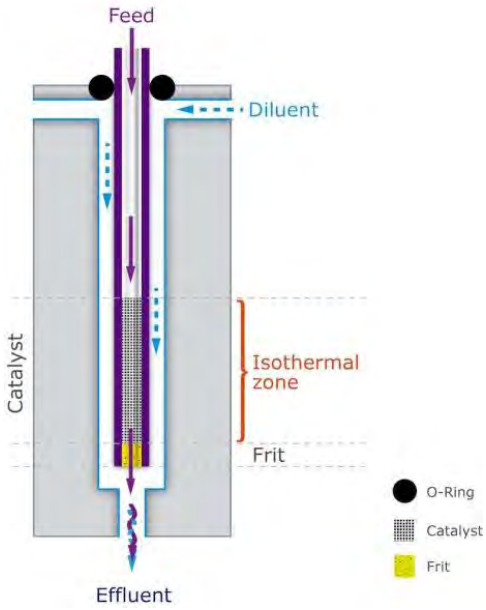

Figure 4-6: Cross-section of reactor with catalyst in heating block.

To prevent a pressure difference inside and outside the reactor tube, specifically when using quartz reactors, a nitrogen diluent flow was used along the outside of the reactor tube. This flow was mixed with the reactor effluent after the reactor tube. Other benefits of diluting the downstream flow with nitrogen is to increase the total flow improving the back pressure regulator workings, as well as to lower the vapour pressure of the effluent compounds (to maintain n gas phase).

All gas and liquid feeds are fed to the reactors without a bypass. To measure the feed composition, required for conversion calculations, at least one reactor is filled with only SiC (no catalyst). This 'empty' reactor is referred to as the blank reactor.

Downstream section

The effluent of each reactor flows downstream to the parallel back pressure regulator. The pressure regulator consists of 16 parallel little compartments with a Teflon membrane divider. On one side of the membrane is the inlet for the reactor effluent and the outlet (to the selection valve). The other side of the membrane has only one port for a nitrogen reference pressure, generated by pressure indicator controller (PIC). The reference pressure will press the Teflon membrane to close the reactor effluent inlet until the pressure in the reactor is equal or slightly higher than the reference pressure. Reactor effluent will flow through the pressure regulator until the reference pressure is again greater than the reactor pressure. The 16 parallel back pressure regulators are controlled through a single PIC, resulting in an equal reactor pressure in all reactors. Figure 4-7 is a schematic drawing of the downstream section as well as the back pressure regulator.

The flow from the parallel pressure regulator goes to a 16-port selected/common selection valve. This valve will select one single reactor and feed the selected flow to the analysis. All other non-selected reactor effluents are directed to the waste through the common port of the selection valve.

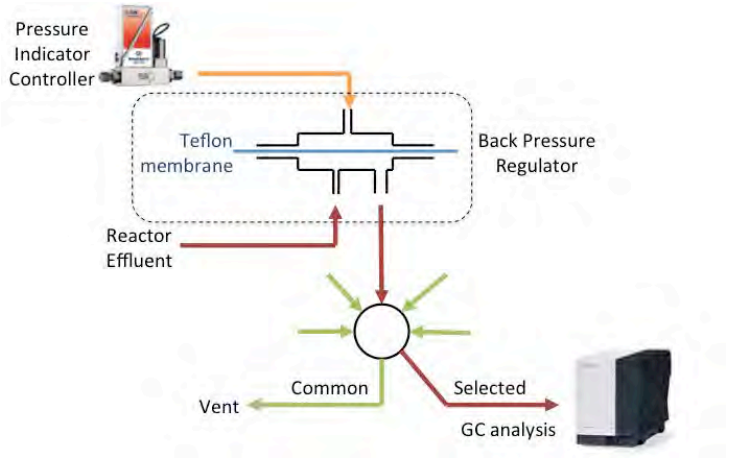

Figure 4-7: Schematic drawing of the parallel back pressure regulator, selector valve and GC analyser.

The effluent of the selected reactor was quantitatively analysed for the known components using a gas chromatography (GC). A Micro-GC from Agilent (CP-490 model) with four columns was used. In a single analysis, all four columns were injected at the same time with the same effluent of the selected reactor. Refer to section 4.3.2 for more details on the GC setup and method used.

The flushing time of the tubing between the switching of the selector valve and the injection on the GC was determined by analysing one reactor multiple times in a row and compare the results. When the first (or first few) analysis deviates it suggests that the flushing time is not sufficient. Due to the relative small tubing in the setup a flushing time of 10 minutes between switching of selector valve and injection of GC was sufficient, and no deviation between the first and subsequent analysis was observed. However, due to the high amount of data a flushing time of 15 minutes was used.

In all experiments the reactors were analysed either one by one, a single analysis of a reactor (reactor 1, 2, 3, 4, etc., 16), or a triplicate, three analyses of each reactor (reactor 1, 1, 1, 2, 2, 2, 3, 3, 3, 4, 4, etc.). The data of the triplicate analysis was used as an averaged data point (of the three) to limit the high amount of data generated. However, the triplicate analyses were checked for irregularities (e.g. issues with flushing time or blocked reactor).

4.3.2 Gas Chromatographic Analysis

The Agilent CP-490 micro gas chromatograph (micro-GC) contains 4 parallel injectors, columns and thermal conductive detectors (TCD). Table 4-1 gives an overview of the components detected on each column.

Water vapour can be detected on both the PoraPLOT Q (PPQ) and CP-Sil 5CB column; however, due to the enormous tailing of the peak quantification is inaccurate. Also, the non-linear response for water vapour by the TCD results in inaccurate quantification. Therefore, no analysis for water was performed.

It should be noted that the analysis method was optimised for this project and not for other compounds. All components in this project were analysed on the MS5 and CP-COX column and no method optimisation for the other columns was required.

Table 4-1: GC setup and the components detected.

Column	Component	Retention time[a] (min)	Response factor[b]
MS5	He[c]	0.96	1
	H_2	1.05	1.21921
	N_2	1.6	
	CH_4	2.15	0.375394
	CO	2.75	0.127041
COX	Unseparated[d]		
	CO	0.9	0.0951073
	CH_4	1.87	0.0842114
	CO_2	4.13	0.134906
PPQ	Unseparated[d]		
	CO_2	0.51	0.430604
	H_2O[e]		
CPSil	CH_4	0.48	
	H_2O[e]		

[a] Retention time depending on method and influenced by column degradation and H_2O and CO_2 injected,
[b] Used in calculations,
[c] Used as internal standard,
[d] The unseparated peak consists of all the unretained components,
[e] Not quantitatively analysed.

Backflush

The MS5 column was equipped with a backflush option to prevent compounds eluting later from a pre-column to reach the analytical MS5 column and detector. The backflush prevents specific compounds getting onto the GC column, e.g. compounds that will damage the column over time. The pre-column is equivalent to a short PPQ column and water can be prevented from reaching the MS5 column, as water will block the molsieve pores. Water can only be removed slowly from the MS5 column at elevated temperatures.

Figure 4-8 shows a schematic drawing of the backflush system employed in the micro-GC. The two columns, pre-column and analytical column, are coupled in series with a pressure point which makes it possible, at a pre-set time, to invert the carrier gas flow direction to 'backflush' the pre-column, while still continuing the carrier flow on the analytical column (Varian Micro-GC User Manual, 2005). The backflush timing is dependent on the setup, method and compounds, and was be determined between the analytical method development and calibration.

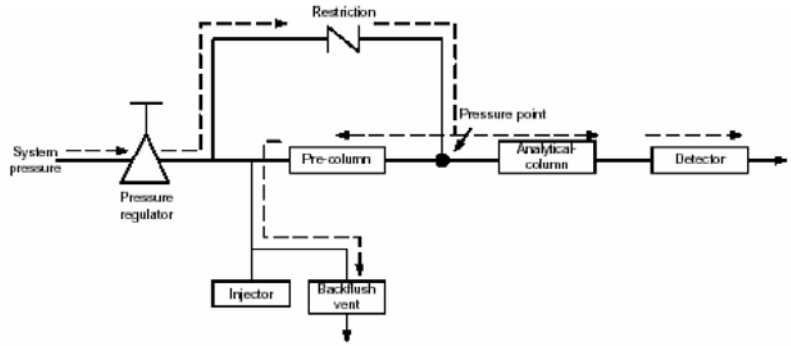

Figure 4-8: Schematic of a backflush setup in the micro-GC (adapted from Varian Micro-GC User Manual, 2005).

Micro-GC method

The analysis methods on the micro-GC have been optimised for separation and detection of the compounds involved in the steam reforming of methane and water-gas shift reaction for fuel processing. Table 4-2 gives the overview of the main parameters of the method. An example chromatogram is included in Appendix 9.3.

Table 4-2: Micro-GC method parameters.

Channel #[a]	**1**	**2**	**3**
Column (length in meters)	**MS5 (20m)**	**COX (1m)**	**PPQ (10m)**
Injector temperature (°C)	109	109	109
Column temperature (°C)	100	80	110
Carrier gas	Argon	Helium	
Carrier pressure (kPa)	250	110	110
Sample line temperature (°C)	110		
Sample line flush time (s)	30		
Injection time (ms)	75	75	75
Backflush timing (s)	11.5	8.5	15
Analysis time (min)	5	5	5

[a] Channel 4 (CPSil column) has been left out as it was not used in this project and the method was not optimized,

[b] Channel 3 (PPQ column) was initially used to verify the consistency of CO_2 detection between the COX and PPQ column.

4.3.3 Calibration

Before the catalyst screening was executed, all the equipment components were calibrated individually. The mass flow controllers (MFC) were first calibrated for the correct flow. Subsequently, the GC was calibrated with a gas mixture made up by the calibrated MFCs. The ranges for calibration were set around the fuel processor model feed and product composition.

Mass flow controller calibration

The mass flow controllers were calibrated for correct flow by using a bubble meter and stopwatch. The flow was measured by displacement of a single soap bubble

through column and a known volume was timed giving actual flow rates. No MFCs did deviate from the set flow, as the supplier previously calibrated the equipment. The correction factors used in the software are noted in Table 4-3 and no additional correction was needed.

Table 4-3: Mass flow controllers' calibration factors.

MFC	Conversion factor
Methane	0.03125
Nitrogen	0.15625
Hydrogen	0.03125
Carbon monoxide	0.003125
Carbon dioxide	0.0078125
Helium	0.0021875
Air[a]	0.00078125

[a] Not used in this project.

The Flowrence equipment uses one pressure indicator controller (PIC). However, no certified pressure indicator was available to calibrate and the supplier values were used (all experiments were run at 1 bar_g).

Gas chromatograph calibration

The quantitative analysis on the micro-GC was calibrated using the above calibrated mass flow controllers (MFC). Gas compositions, to model the feed and product ranges, were mixed by the MFCs and analysed on the micro-GC (Table 4-4).

Table 4-4: Model effluent gas composition for micro-GC calibrations.

X_{CH4} (%)	Set MFC flows (Sml/min)				
	H_2	CH_4	CO	CO_2	He[a]
0		273			27
50	478	136	68	68	27
75	478	46	68	68	18
25	239	205	34	34	27
60	573	109	82	82	27
80	510	36	73	73	18
15	143	232	20	20	27

[a] Used as internal standard.

Numerous analyses were obtained for each model gas composition and averaged for use in the calibration (Table 9-1 and Table 9-2 in appendix 9.4). The analysis obtained from the hydrogen in the calibration is plotted in Figure 4-9, where the H_2 measured areas is plotted versus the H_2 concentration. The linear line suggests a linear response of H_2. Similar, the other components (CH_4, CO and CO_2) all show a linear response on all the columns (MS5, COX and PPQ), see appendix 9.4.

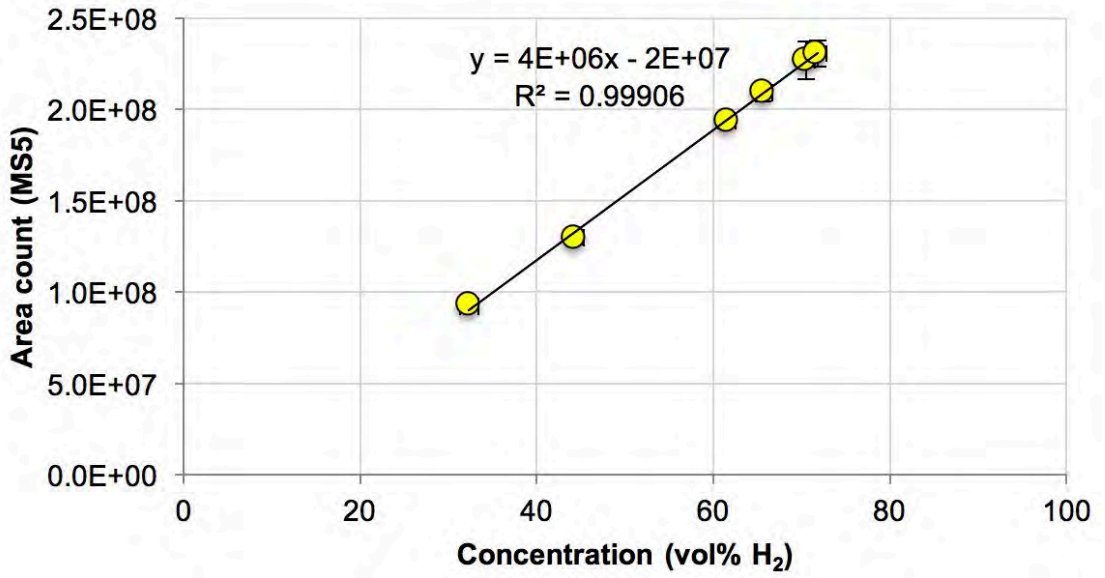

Figure 4-9: Micro-GC calibration of hydrogen.

Temperature calibration for isothermal reactor zone

For each heating block the temperature was measured to determine the isothermal zone for correct catalyst loading. This was performed at two temperatures, 300°C for WGS reaction and 900°C for steam reforming. It is assumed that the isothermal zone below 300°C is similar.

The measurements were performed for one reactor position at each heating block. A thermal couple with digital handheld reader was used to measure the temperature at various distances in the reactor position. All the heating blocks were set to respectively 300 and 900°C, hold for at least one hour before measurement. The measurements were taken at specific distances from the top and after each recording the thermal couple was placed lower into the heating block and hold to stabilize. It should be noted that the used thermal couple and handheld reader were not calibrated. The thermal couple might not measure the precise temperature, however, the thermal couples were assumed to be accurate in deviation.

The accepted variation for isothermal zone is a maximum deviation of ± 1°C. Figure 4-10 and Figure 4-11 show the measured results and the defined isothermal zones for all heating blocks.

4.3.4 Data work-up and calculations

The work-up of the raw data (peak areas and process conditions) and calculations were performed using Microsoft Access database. All raw data, peak areas from the micro-GC analysis and the process data from the Flowrence, were matched on time. The resulting data set was filtered for outliers (e.g. integration errors, pressure fluctuation, blocked reactor) before calculations were made.

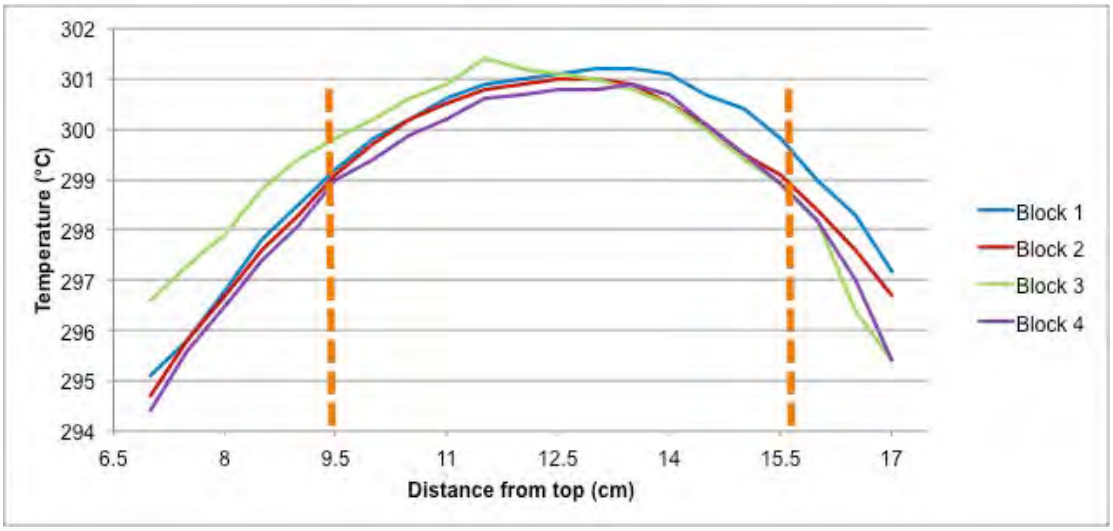

Figure 4-10: Isothermal zone measurement for all heating blocks at 300°C.

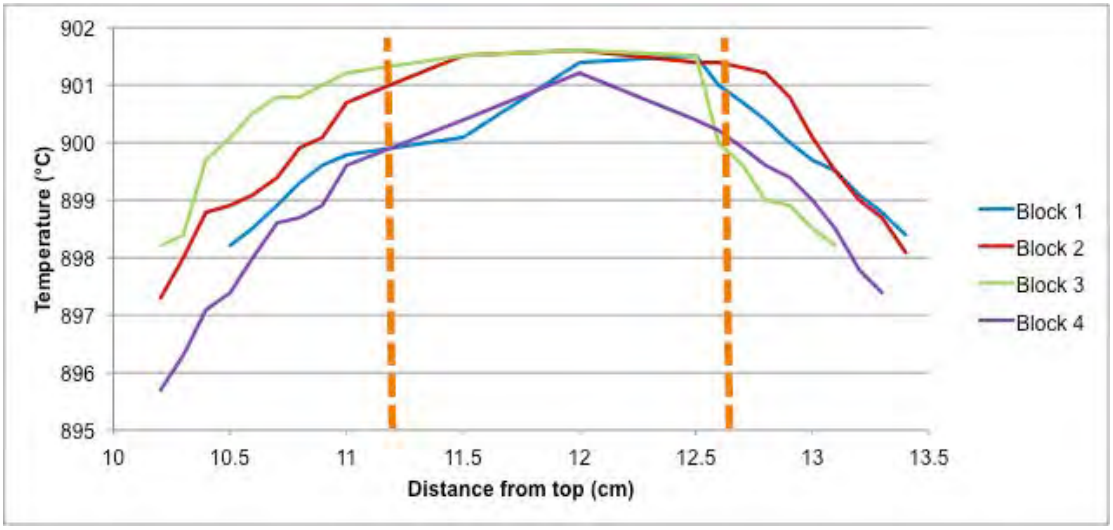

Figure 4-11: Isothermal zone measurement for all heating blocks at 900°C.

The feed composition was calculated using the blank reactors. This 'blank' data was used in the calculations as the feed composition and flows. To minimise the fluctuation of the nitrogen diluent and deviations in injection sample volume an internal standard, helium, was mixed in the feed composition and expected not reactive. Each micro-GC channel uses the same principle of injection (based on pressure difference between sample line and carrier), assuming consistent injection volumes between the GC channels (i.e. if larger volume was injected on column 1, the same relatively larger volume was also injected on the other columns, as the pressure in the sample line is the same). Therefore, the area of the internal standard on the MS5 channel can be used in the calculation for the components on the COX channel.

For each component a response factor was calculated between the compound *i* and helium as the internal standard. Equation 4-1 was used to calculate the response factor (Rf_i) of compound *i*, the concentration (volume percentage) divided by the area, both normalised to the internal standard.

Equation 4-1: Calculation response factors based on internal standard.

$$Rf_{i/He} = \frac{\frac{vol\%_i}{vol\%_{He}}}{\frac{Area_i}{Area_{He}}} \qquad vol\%_i = \text{volume per cent compound } i$$

The conversion (X_i) of CH_4 in steam reforming and CO in water-gas shift reaction is calculated using Equation 4-2. The *out* referring to the effluent and the *in* refers to the analysis of the 'blank' reactor.

Equation 4-2: Conversion of compound *i*.

$$X_i = \frac{\frac{Area_i^{out}}{Area_{He}^{out}}}{\frac{Area_i^{in}}{Area_{He}^{in}}} \cdot 100\% \qquad X_i = \text{Conversion of compound } i$$

To describe the reproducibility of a series of data points (e.g. the conversions of a set of reactors) the standard deviation is calculated using Equation 4-3. The standard deviation was expressed as relative standard deviation (RSD), a percentage of the average value (Equation 4-4).

Equation 4-3: Standard deviation calculation.

$$\text{Standard deviation} = \sqrt{\frac{\sum(x - \bar{x})}{(n-1)}}$$

Equation 4-4: Relative standard deviation.

$$\text{RSD} = \frac{\text{standard deviation}}{\text{average}} \times 100\%$$

4.3.5 WGS reproducibility

In the water-gas shift study two different types of catalysts have been tested. The commercial catalyst was a low temperature shift (LTS) CuZn catalyst (commercial catalyst code is ShiftMax240) and is known to be very sensitive to fast reductions and high temperatures. Typically, in industry this CuZn catalyst is used between 190 and ~230°C, where the temperature slowly increases over time to compensate for the deactivation.

The second catalyst group for the WGS study was the platinum group metal (PGM) catalyst Pt/Al_2O_3. This catalyst was prepared on the Chemspeed platform in 8 batches all with 1 wt% metal loading. The catalysts were prepared following the incipient wetness impregnation (refer to section 4.1.2). The PGM catalysts were more stable at higher temperatures but less active then the CuZn catalyst. Therefore, the temperature range tested was higher.

Base metal catalyst $CuZn/Al_2O_3$

The following steps were performed to activate the $CuZnO/Al_2O_3$ catalysts before reaction conditions. The same activation steps were performed during the run when the reactors were exposed to air for changing reactor positions and the experiment was re-started.

- Flush with N_2 to remove air from the reactor
- Feed 3.8 vol% H_2 in N_2 with a GHSV of 475 000 h^{-1}
- Heat up to 204°C at 1°C/min and hold for 16 hours
- Feed 100% H2 at 204°C for 1 hour
- Decrease the temperature to 200°C (reaction temperature)
- Slowly pressurize reactor to 20 bar_g at 1 bar/min
- Start dry gas feed (H_2, CO, CO_2) and steam (H_2O) simultaneously at the space velocity of the first reaction condition (40 000 h^{-1}) and feed composition as in Table 4-5.

Table 4-5: Feed composition for commercial LTS catalyst.

	Set point (Sml/min/reactor[a])	Feed composition (vol%)
H_2	17.5	40
CO	0.75	2
CO_2	4.25	10
H_2O	1.4	43
He	1.25	3
N_2	1.25	3

[a] Standard millilitres per minute per reactor

Platinum group metal catalyst Pt/Al_2O_3

Similar to the initial start-up of the base metal catalyst, the following procedure was used for the Pt catalysts in WGS:

- Flush with N_2 to remove air from the reactor
- Feed ~10 vol% H_2 in N_2
- Heat up to 300°C at 2°C/min
- Feed 100% H2 at 300°C for 90 minutes
- Slowly pressurize reactor to 1 bar_g and start steam
- Start dry gas feed (H_2, CO, CO_2) at the space velocity of the first reaction condition and feed composition as in Table 4-6 and Table 4-7.

The Pt catalyst experiments were performed with a model feed composition representing reformate stream in a fuel processor (Table 4-6). During the experiment

various conditions were tested, Table 4-7, but the feed composition remained unchanged.

Table 4-6: Feed composition for fuel processing reformate.

	Feed composition (vol%)
H_2	50
CO	7.5
CO_2	6.5
H_2O	33.3
He	2.8

Table 4-7: Condition steps in WGS many-to-many experiment.

Condition step	Temperature (°C)	SGHSV (h^{-1})
1	300	15 000
2	325	15 000
3	350	15 000
4	350	10 000
5	350	5 000
6	350	15 000

4.3.6 SMR reproducibility

Similar as in the WGS study, two experiments were performed for steam methane reforming (SMR), but now at the required high temperature of 700°C. In the first experiment, one-to-many, a single catalyst batch is prepared on the Chemspeed and tested in multiple reactors on the Flowrence. In the following many-to-many experiment, eight batches of catalyst were prepared and tested on the Flowrence for their conversion activity. The catalysts used in both these SMR experiments were 0.5 wt% Rh/Al_2O_3 (target metal loading).

The steps below were followed to activate/start-up of the SMR experiments.

- Flush with N_2 to remove air from the reactor
- Feed 100% H_2 (at low space velocity)
- Heat up to 750°C at 1°C/min and hold for 2 hours
- Start the steam and decrease the temperature to 700°C (reaction temperature) at 1°C/min; hold for 30 min
- Stop H_2 and start CH_4 feed at the space velocity of the first reaction condition and feed composition as in Table 4-8; hold for 30 min

- Slowly pressurize reactor to 1 bar_g and hold for 30 min.

The one-to-many experiment was started at a SGHSV of 50 000 h^{-1} and the space velocities where increased twice over time (see Table 4-8 for the conditions). The many-to-many experiment was performed at condition 3 only (Table 4-8) and no changes were made over time.

Table 4-8: Condition steps for SMR experiment.

Condition	Temperature (°C)	S/C[a]	SGHSV (h^{-1})
1	700	3	50 000
2	700	3	75 000
3	700	3	115 000

[a] Steam to carbon ratio

5 Results

This project aims to validate the high throughput experimentation equipment for fuel processing catalysts development. A great number of catalysts have been prepared using robotic synthesis equipment and subsequently tested in parallel fixed bed reactors. In this study, the fuel processing reactions that were selected as case studies were steam methane reforming and water-gas shift. The catalysts prepared for steam methane reforming (SMR) were 0.5 wt% Rh/Al_2O_3 and for water-gas shift (WGS) were 1 wt% Pt/Al_2O_3. These are both formulations known to be highly active in the fuel processing reactions, however, they are not optimised for each reaction (outside the scope of the project). The main focus was placed on the reproducibility of the high throughput equipment for preparation and testing and only partly on characterisation analysis.

5.1 Catalyst characterisations

For this project three catalysts were used; a commercial catalyst and two PGM catalysts prepared by incipient wetness impregnation, viz. Pt/Al_2O_3 and Rh/Al_2O_3. The commercial catalyst comes with an agreement that no characterisation may be performed on it. Due to slow throughput of the analytical measurements and the long equipment times required, only limited characterisations were performed on the Pt & Rh/Al_2O_3 catalysts to support this study.

5.1.1 Pt/Al_2O_3 characterisations

CO Chemisorption was performed on the Pt/Al_2O_3 catalyst series used in the WGS many-to-many experiment. Catalysts from two impregnation series were analysed, one single catalyst batch and a series with 8 batches. All batches of impregnated Pt/Al_2O_3 were prepared using the same recipe settings on the Chemspeed and were aimed for 1 wt% Pt loading.

The results from the CO chemisorption of the Pt/Al_2O_3 are presented in Figure 5-1. The single batch (internal catalyst code FP0104) was analysed twice on different days to get a feel for the precision of the analysis. The first two data points in Figure 5-1 are from the FP0104 catalyst batch. The other eight batches are prepared in one series in parallel.

Some discrepancy between the two analysis of catalyst FP0104 is observed, see also Table 5-1. This variation can be caused by the instrument error or, more likely, an inaccuracy in the weighing of small amounts. Nonetheless, all other batches gave results within the spread of the FP0104 analysis.

Table 5-1 also contain the ICP (inductively coupled plasma - optical emission spectrometer) results. The batch number 2 through 9 were prepared from a single Pt salt stock solution and variation on the Pt loading can be introduced by errors in concentrations of the impregnation solutions, differences in volume of impregnation solution added to the support or errors in the ICP analysis. The catalyst samples were completely dissolved before the ICP analysis and diluted to concentrations within the calibrated ranges on the instrument.

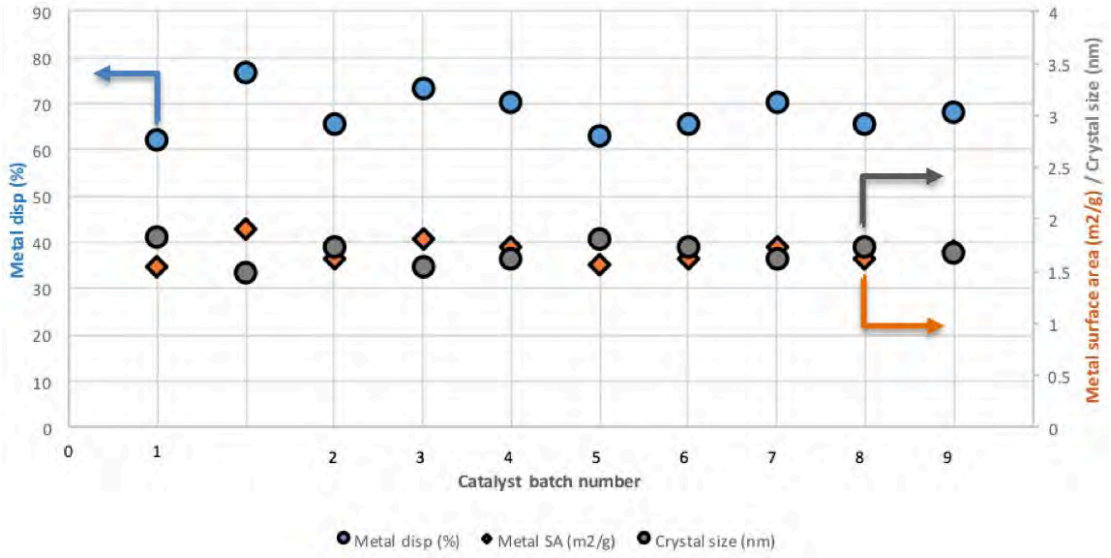

Figure 5-1: CO chemisorption of Pt/Al_2O_3 catalyst series.

Table 5-1: CO chemisorption and ICP-OES analysis of Pt/Al_2O_3 catalyst batches.

Batch number	Catalyst ID[a]	Metal wt%[b]	Metal disp[c] (%)	Metal SA[d] (m^2/g)	Crystal size (nm)
1	FP0104[e]	1.22	62	1.53	1.83
	FP0104[e]		77	1.90	1.47
2	FP0150	0.96	65	1.62	1.73
3	FP0151	0.85	73	1.81	1.55
4	FP0152	1.05	70	1.73	1.62
5	FP0153	1.07	63	1.55	1.80
6	FP0154	1.03	65	1.61	1.73
7	FP0155	0.96	70	1.73	1.61
8	FP0156	1.15	65	1.62	1.73
9	FP0157	0.88	68	1.68	1.66
Average[f]		*1.02*	*68*	*1.68*	*1.67*
RSD[g]		*11.8%*	*6.86%*	*6.86%*	*6.67%*

[a] Catalyst batch identification number (used internally).
[b] ICP analysis.
[c] Metal dispersion.
[d] Metal surface area (SA).
[e] Single catalyst batch analysed once for ICP and twice for chemisorption at different days.
[f] Average value of the 10 catalyst analysis.
[g] Relative standard deviation (RSD) of the 10 catalyst analysis.

5.1.2 Rh/Al_2O_3 characterisations

In the steam methane reforming study, a Rh/Al_2O_3 was used. Two studies were performed on the high throughput equipment and can be divided in a one-to-many and a many-to-many experiment. In the one-to-many experiment, one catalyst batch was prepared. In the many-to-many experiment, 8 batches of 0.5 wt% Rh/Al_2O_3 were prepared. These catalysts were analysed for the metal loading through ICP analysis.

To determine the reproducibility of the ICP-OES analysis itself, the single catalyst batch was analysed 6 times as duplicates (6 samples of a single catalyst batch were used for 6 analyses). The expected rhodium loading was 0.5 wt% and the ICP analysis confirmed the loading (Table 5-2). The relative standard deviation is 3.9% of the average.

Table 5-2: Duplicate ICP measurements of 0.5 wt% Rh/Al_2O_3.

Catalyst ID[a]	Sample mass[b] (mg)	Rh content (wt%)
FP0017	204.7	0.49
	208.7	0.49
	214.9	0.50
	204.3	0.49
	200.2	0.54
	201.4	0.51
Average		***0.50***
RSD		***3.9%***

[a] Catalyst batch identification number (used internally).
[b] Sample weight used for analysis.

The Rh catalysts for the many-to-many experiment were analysed for the variation in impregnation by the Chemspeed synthesis robot. The rhodium metal content in the 8 prepared catalyst batches were analysed by ICP-OES and the results are given in Table 5-3.

The intended rhodium loading for this series was 0.5 wt% for each catalyst, and although the ICP indicates 0.4 wt%, the reproducibility in the preparation remains good. The small deviation from the intended loading can be explained by a low Rh metal content in the salt, additional adsorbed water (hygroscopic property of the salt), or a systematic error in the analysis itself. Though, the RSD of the series is within agreement of the RSD of duplicate measurement.

Table 5-3: ICP analysis of Rh/Al_2O_3 series for the many-to-many experiment.

Catalyst ID[a]	Sample mass[b] (mg)	Rh content (wt%)
FP0023	230.2	0.38
FP0024	201.6	0.38
FP0025	201.4	0.42
FP0026	204.1	0.39
FP0027	101.0	0.55
FP0028	209.5	0.42
FP0029	211.8	0.42
FP0030	215.9	0.41
Average		***0.40***
RSD		***4.7%***

[a] Catalyst batch identification number (used internally).
[b] Sample weight used for analysis.

5.2 WGS reproducibility

The validation for the high throughput equipment under 'mild' water-gas shift conditions was first performed using a commercial low temperature shift (LTS) catalyst. Within this LTS study the validation in the reactor position was also assessed. Further, the results of the catalyst preparation were validated by preparing 8 times a Pt/Al_2O_3 catalyst in parallel and tested for the WGS activity.

5.2.1 Commercial catalyst

Initial validation of the parallel fixed-bed equipment was performed using commercial water-gas shift (WGS) catalyst. The catalyst used was a commercial low temperature shift catalyst comprising of CuZn supported on alumina (Shiftmax240). This catalyst is known to be highly active around 190 – 230°C and tests were performed at 200°C under typical industrial water-gas shift conditions. Each reactor was charged with the same mass of catalyst (appendix 9.5) and a deviation of 1.7 mg between the lowest and highest catalyst loading (RSD = 0.74%) was obtained.

The results obtained showed all catalysts required time to settle in and activities stabilised between 35 and 43% CO conversion (Figure 5-2).

To confirm that the variations in activities are not equipment related, the run was interrupted and the reactor tubes were moved to different positions in the high throughput platform. After 110 hours on stream the run was interrupted (cooled down under inert gas feed) to change the reactors in the block positions. The reactor with the lowest activity was swapped for the reactor with the highest activity; the second lowest activity was then changed to the position of the second highest, etc. Reactor positions were changed within the heater blocks and between heater blocks. It must be noted that the complete reactor tubes, including the catalyst, were exchanged from positions. Table 5-4 shows the reactors initial reactor position (ToS < 110h) and the new positions (ToS > 150h).

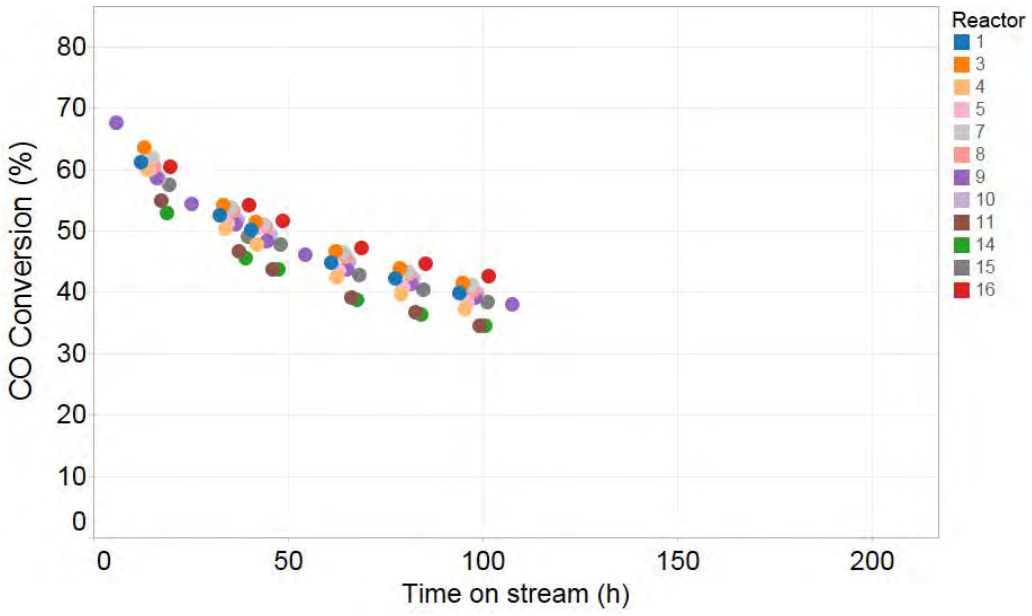

Figure 5-2: Conversions of commercial low temperature shift catalyst; 200°C, SGHSV 40 000 h^{-1}, 20 bar_g, feed composition in section 4.3.5.

Table 5-4: Changed reactor positions.

Reactor (ToS < 110h)	Catalyst Name[a]	CO conversion[b] (% at ToS < 110h)	Reactor (ToS > 150h)	Catalyst Name[a]
1	ShiftMax240	39.8	13	Blank
2	Blank		5	ShiftMax240
3	ShiftMax240	41.1	11	ShiftMax240
4	ShiftMax240	37.1	7	ShiftMax240
5	ShiftMax240	38.2	2	Blank
6	Blank		9	ShiftMax240
7	ShiftMax240	40.7	4	ShiftMax240
8	ShiftMax240	40.2	15	ShiftMax240
9	ShiftMax240	39.0	6	Blank
10	ShiftMax240	39.7	12	Blank
11	ShiftMax240	34.2	3	ShiftMax240
12	Blank		10	ShiftMax240
13	Blank		1	ShiftMax240
14	ShiftMax240	34.1	16	ShiftMax240
15	ShiftMax240	38.2	8	ShiftMax240
16	ShiftMax240	42.4	14	ShiftMax240

[a] ShiftMax240 is a commercial low temperature water-gas shift catalyst containing CuZn supported onto Al_2O_3.

[b] Conversion at the last data point taken before reactor positions were changed.

After changing the positions of the reactors, the run was re-started again by re-reducing all catalysts and subsequent activity measurements of WGS activity. It is

important to note that a similar procedure was followed for the re-start as for the initial start-up, however, the time on stream was calculated as t_0 = 0 h initial start-up.

In this experiment the reactor and its position should be considered as different variables. The position refers to the location in the heating block and the reactor refers to the tube that contains the catalyst. Therefore, a reactor can be placed in any of the 16 positions.

The data shown in Figure 5-3 are the conversions for reactor number 14 and 16, two reactors that the positions were exchanged (reactor 14 was moved to position 16 and vice versa). The reactors are represented by colour and the position by shape. The activity of reactor 16 is slightly higher than reactor 14. After exchanging the position, the reactor 16 (red) remains at a higher activity then reactor 14 (green). Similar patterns are observed for the other exchange of reactors, within a heating block as well as between heating blocks. This suggests that the variation in conversion is reactor, or catalyst loading, related and not due to the equipment.

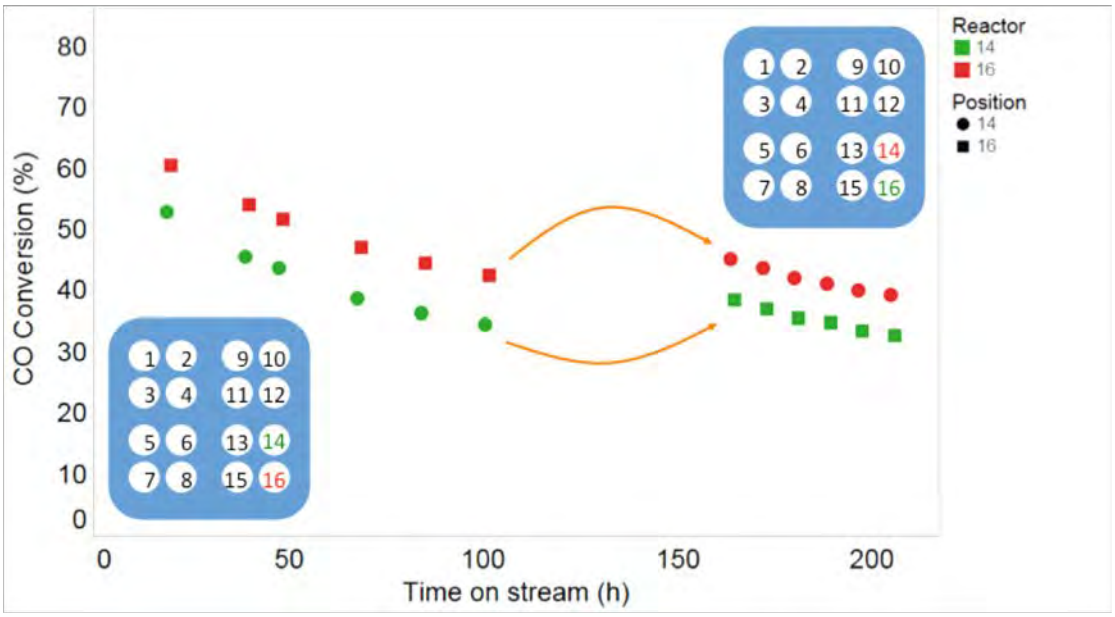

Figure 5-3: Conversions of reactor 14 and 16, before and after position change; 200°C, SGHSV 40 000 h^{-1}, 20 bar_g, feed composition in section 4.3.5.

From the data of the single commercial catalyst in multiple reactors a relative standard deviation (RSD) can be calculated. The data set used for this calculation included only the last analysis of each reactor before exchanging reactors, as this condition is nearing stable performance. Figure 5-4 marks the dataset used. The average conversion was 38.8% ± 2.4, making the RSD 6.3% of the average.

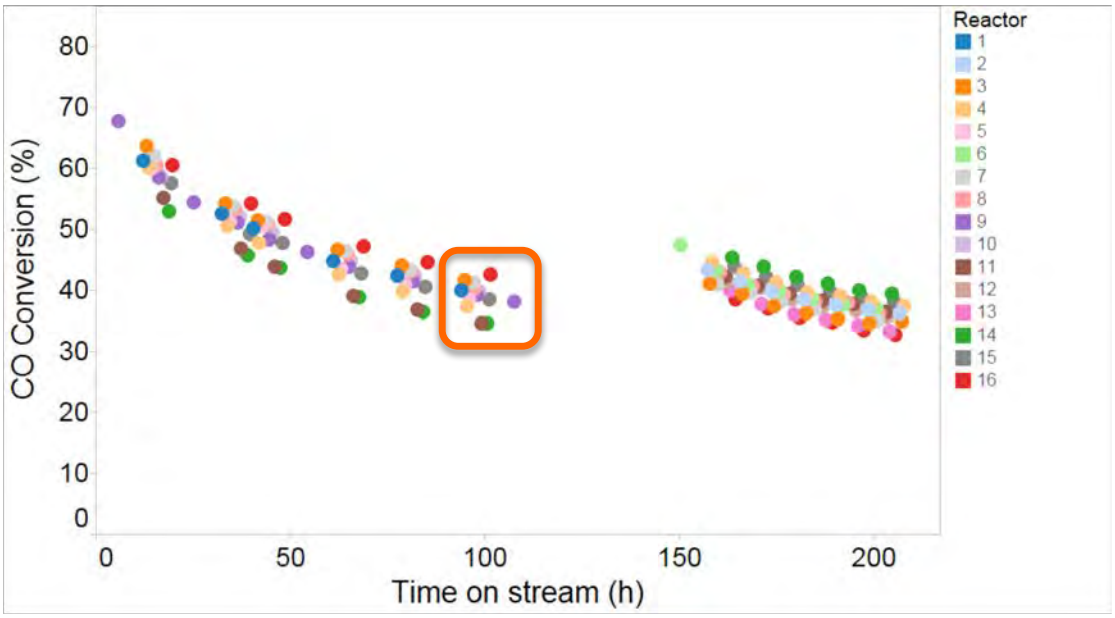

Figure 5-4: Data set for RSD calculations; 200°C, SGHSV 40 000 h^{-1}, 20 bar_g, feed composition in section 4.3.5.

5.2.2 Many-to-many

Using the Chemspeed synthesis robot impregnations were performed to prepare eight batches of 1 wt% Pt/Al_2O_3 catalyst. From the ICP analyses (section 5.1.1 and Table 5-1) the metal loading was found to be within acceptable variations. Each batch of the Pt/Al_2O_3 catalyst was loaded into a reactor on the Flowrence and tested for CO conversion in the WGS reaction. The conditions tested were varied between a SGHSV of 5 000, 10 000 and 15 000 h^{-1}, and temperatures of 300, 325 and 350°C in order to measure the catalyst performances at different levels of conversion (Figure 5-5). The feed composition was a typical reformate stream.

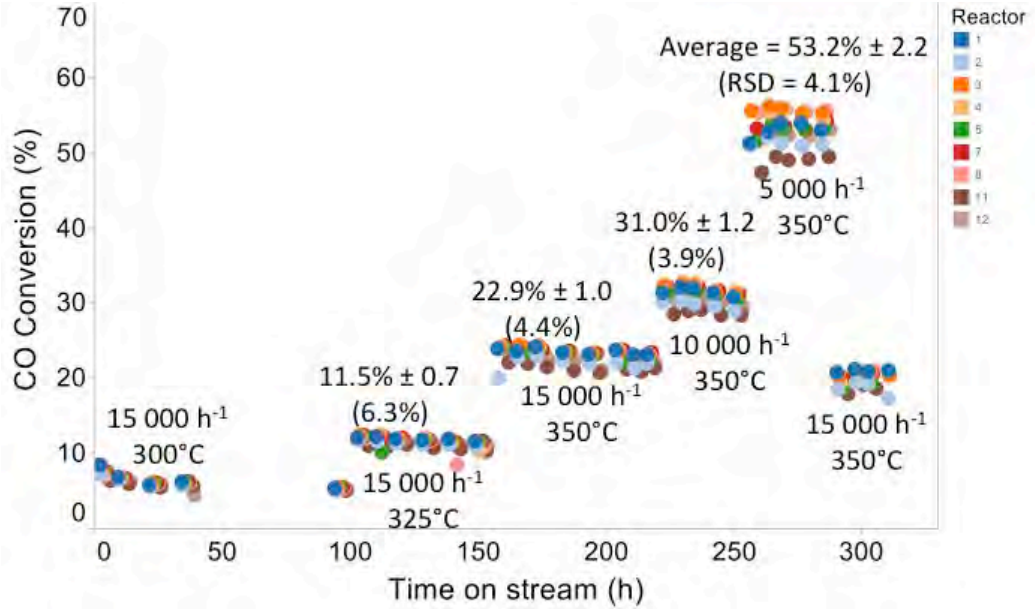

Figure 5-5: WGS activity for the many-to-many experiment using eight batches of 1 wt% Pt/Al_2O_3; temperature and SGHSV noted in figure, feed composition in section 4.3.5.

The relative standard deviation (RSD) at ~50% CO conversion was 4% of the average conversion. This is in accordance with the deviations found with the commercial catalyst. Even at lower conversions the RSD was found to be around 4%. Only at the very low CO conversions of 11% the RSD increased to 6.3%. This was likely due to the inaccuracy on the GC detection of the late eluting CO peak on the MS5 column.

In the final step of the experiment the conditions were changed back to 15 000 h^{-1} and 350°C to check for deactivation. The average conversion of 22.9% decreased to 20% over a period of almost 100 hours and was considered not significant deactivation for these calculations (roughly 1.5% of the total activity was lost per hour).

5.3 Steam methane reforming reproducibility

A similar reproducibility study, as the CO conversion in WGS, was performed for the steam reforming of methane. However, the steam reforming of methane is a highly endothermic equilibrium reaction and requires high temperatures to reach high conversions. Typically, steam methane reforming (SMR) is performed at temperatures between 600 and 900°C. For use in a fuel processor the temperature of 700°C was selected to obtain high enough conversions (at equilibrium).

Similar to the WGS study, various studies were performed to determine the reproducibility of catalyst preparation and screening. All the SMR tests were performed using in-house prepared PGM catalysts.

5.3.1 One-to-many

The first reproducibility study on SMR was performed using a single catalyst batch in multiple reactors (one-to-many) to investigate the deviation in the equipment (between reactors). 12 reactors were charged with a single batch of 0.5 wt% Rh/Al_2O_3 and methane conversions were measured at 700°C. Initially, the SGHSV was set to 50 000 h^{-1}, however, this resulted in conversions very near to equilibrium. Subsequently, the SGHSV was increased to 75 000 h^{-1} and 115 000 h^{-1} to lower the activity and limit influences from equilibrium (without changing the temperature or S/C ratio, which changes the equilibrium conversion).

In Figure 5-6 the methane conversions are plotted versus the time on stream for the three SGHSV. At 115 000 h^{-1} the average conversion dropped to 73% and the relative standard deviation over the marked data points (three GC analyses of all reactors) was calculated to be 2.7% of the average conversion. The data set taken for the relative standard deviation (RSD) calculation was considered to be at stable catalytic conditions. Only very slightly deactivation was observed over the next 150 hours on stream (from 73 to ~70%).

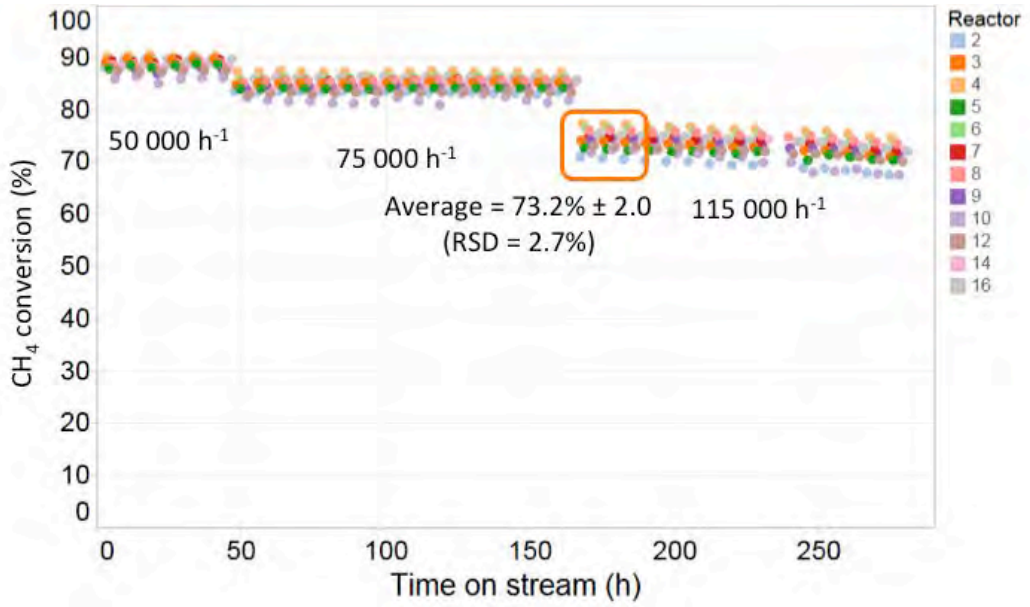

Figure 5-6: One-to-many screening on steam methane reforming; 700°C, S/C = 3, marked data points used for RSD calculations.

5.3.2 Many-to-many

Eight batches of 0.5 wt% Rh/Al_2O_3 were prepared through incipient wetness impregnation using the Chemspeed. The ICP analysis of this series is given in section 5.1.2 and the average rhodium loading is 0.4 wt% ± 0.47%.

The eight batches of Rh/Al_2O_3 catalysts were charged into thirteen reactors, making a many-to-many reproducibility, including some duplicate loadings. The reactor loading can be found in appendix 9.5. The catalyst activities were measured at SGHSV of 120 000 h^{-1} from the start of the experiment. The results are given in Figure 5-7 and show no initial line-in time required for the catalysts. Only over long times on stream a slight decrease in activity was observed. This decrease was equal for all the reactors in the experiment and similar to the data obtained in the one-to-many experiment.

For the deviation calculations three analysis of each reactor between 150 and 200 hours on stream was used (dataset marked in Figure 5-7), corresponding to a similar dataset used in the one-to-many experiment. The RSD for the many-to-many experiment is 3.8% of the average methane conversion of 72.5%.

The steam reforming catalysts show slight deactivation at methane fuel processing conditions over long times on stream. The high temperature of 700°C could possibly cause the Al_2O_3 support to loose surface area and induce sintering of the rhodium metal. Also, slow deposits of carbon formation on the catalyst surface will have a negative influence on the activity over time. The exact cause of the deactivation has not been studied in this project.

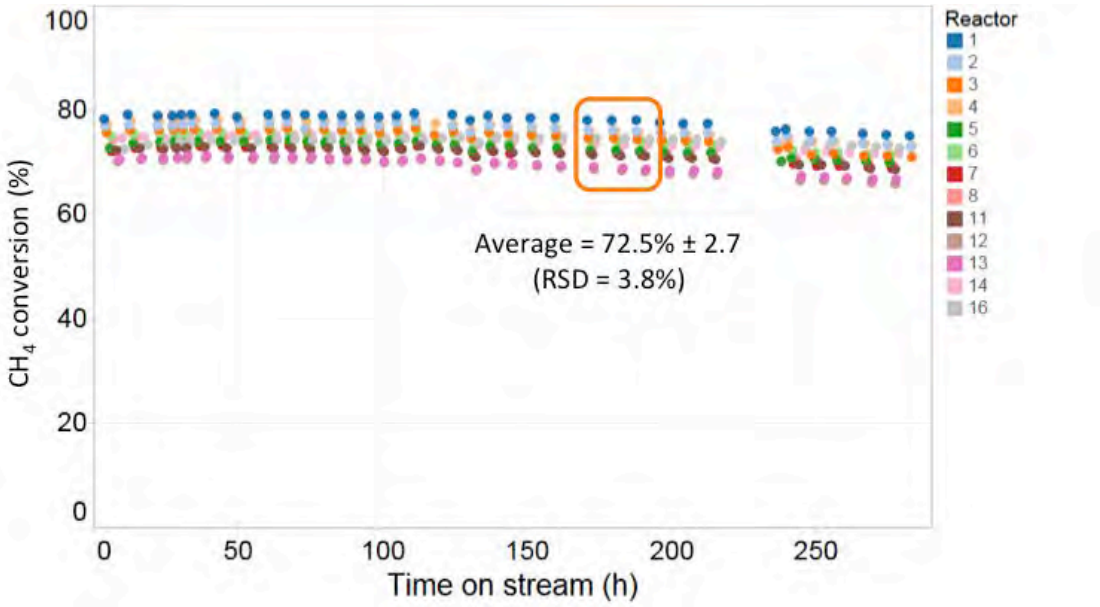

Figure 5-7: Many-to-many reproducibility for steam methane reforming; SGHSV 120 000 h^{-1}, 700°C, S/C = 3, marked data points used for RSD calculations.

5.3.3 Run-to-run

The data for the one-to-many and many-to-many experiments were compared at the same SGHSV. In Figure 5-8 the blue data points are data collected from all reactors in the one-to-many experiment at the highest SGHSV (115 000 h^{-1}), orange data points are from the reactors of the many-to-many experiment (SGHSV is 120 000 h^{-1}). The two experiments give very similar methane conversion, with the spread in the orange data points (many-to-many) being only slightly bigger. Even, the slight deactivation occurring over time had exactly similar trends. This might indicate that the deactivation is dominated by temperature influences over time, suggesting sintering instead of carbon deposition as the primary decomposition mechanism.

Alumina supported rhodium catalysts was prepared in various batches, using high throughput and conventional glassware, and included in various steam reforming studies reference catalyst. This data was collected to compare the overall reproducibility of the high throughput technique compared to conventional testing methods.

Two batches of 0.5 wt% Rh/Al_2O_3 were prepared using the Chemspeed. Both batches, FP0017 and FP0105, were prepared on different days. However, both were prepared and tested according to the same procedure (programme on Chemspeed).

A batch of 0.5 wt% Rh/Al_2O_3 was prepared in conventional glassware by IWI following similar steps as the Chemspeed programme (catalyst code used is PM21).

All catalysts were tested at 700°C and a SGHSV = 200 000 h^{-1}. Catalyst FP0017 was also tested in a conventional single reactor setup (same experimental procedure and conditions). Figure 5-9 shows that methane conversions for these experiments with consistent catalyst behaviour (slight deactivation over long times on stream) and corresponding activities. Only the conventional reactor (square blue data points) show somewhat lower activities.

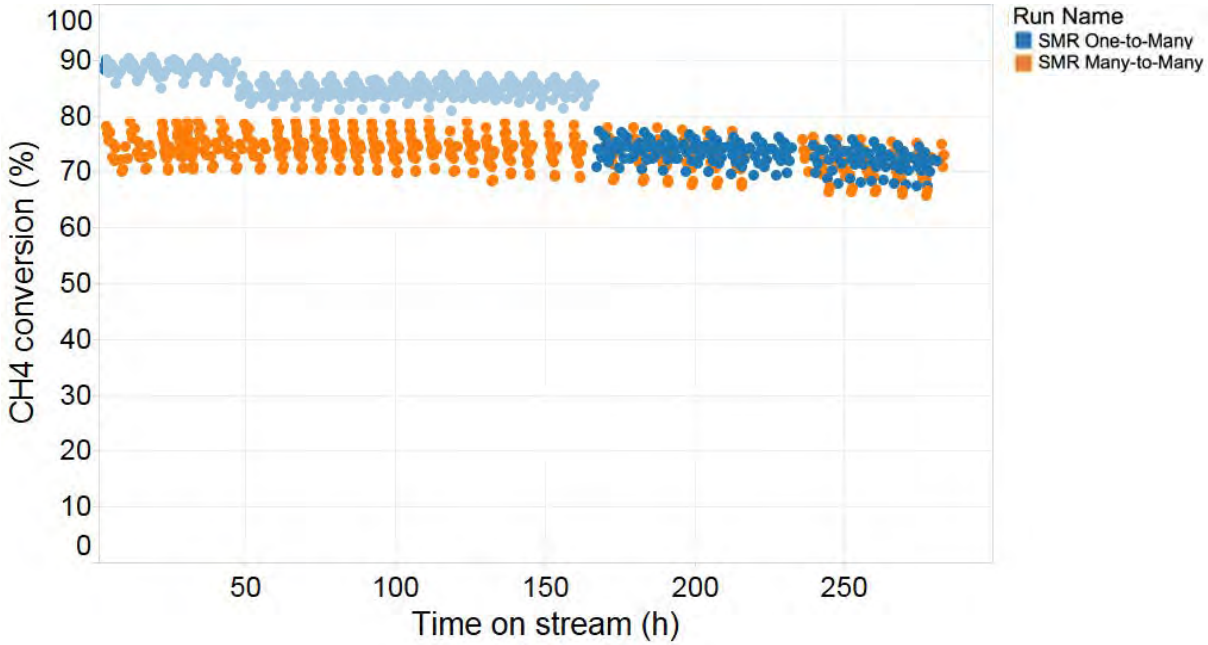

Figure 5-8: Data from one-to-many and many-to-many experiments with similar SGHSV; blue data from one-to-many, orange data collected from many-to-many, SGHSV 115 000 – 120 000 h^{-1}, 700°C, S/C = 3.

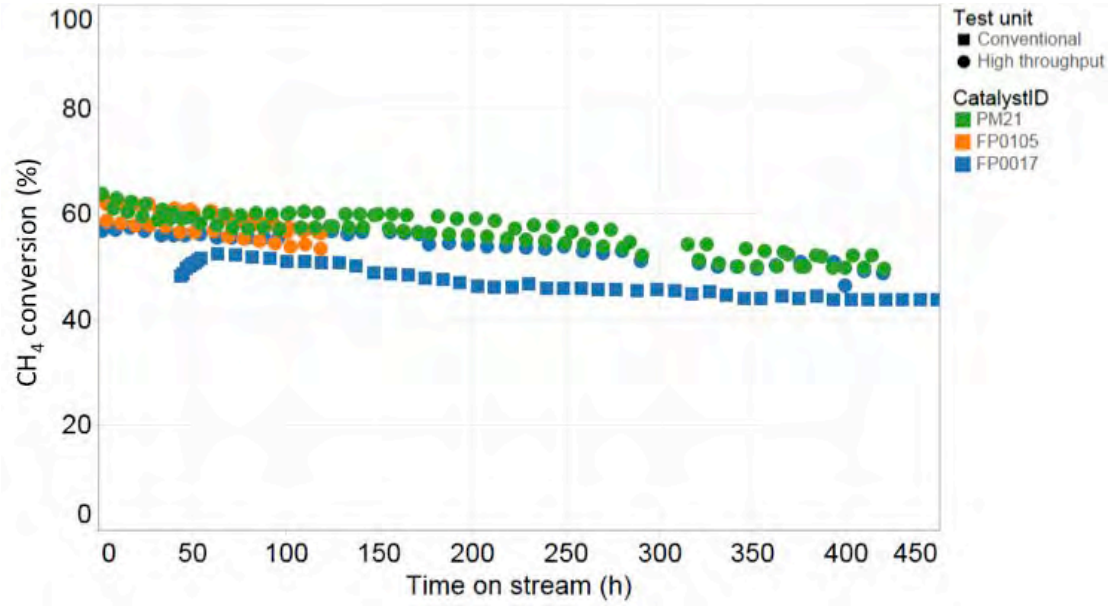

Figure 5-9: Various SMR activity experiments using Rh/Al_2O_3; Conventional reactor is single reactor with ID 16 mm, high throughput is using the Flowrence equipment (circular symbols), colour by catalyst preparation batches, 700°C, SGHSV ~ 210 000 h^{-1}, S/C = 3.

5.4 Influence on metal loading for SMR activity

Rhodium supported alumina catalysts were used for the validation studies and are known to be highly active for the steam reforming of methane. However, often researchers tend to use a 1 wt% Rh/Al_2O_3 and not much data exists on optimising

the metal loading. A study was performed using a range of low metal loadings of Rh deposited on alumina. From the steam reforming validation experiments it was observed that 0.5 wt% Rh/Al_2O_3 was very active and the metal loading range was selected from 0.05 wt% to 0.6 wt%. These catalysts were prepared on the Chemspeed. The activity tests for steam methane reforming were performed at 700°C, steam to carbon ratio (S/C) of 3, and high standard gas hourly space velocities (SGHSV). Figure 5-10 shows the data collected for 8 catalysts for 3 SGHSV, namely 75 000, 150 000 and 225 000 h^{-1}. Specifically low Rh loadings, required approximately 40 hours line in time before a stable conversion is reached.

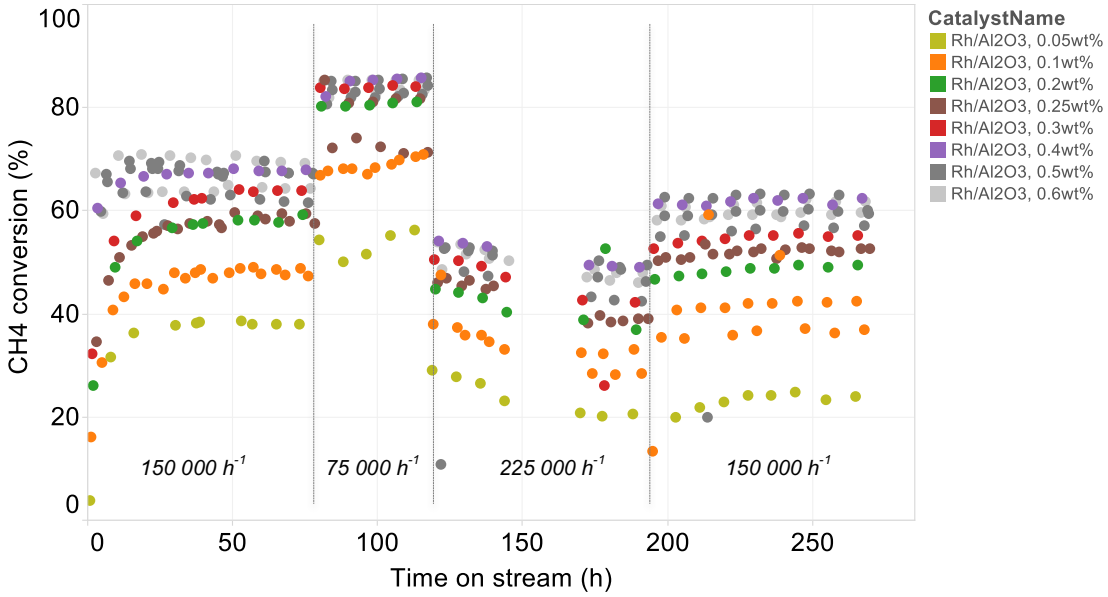

Figure 5-10: Time on stream for steam methane reforming of Rh/Al_2O_3 with various metal loadings; (a power cut was experienced from ToS 150-170h).

Unfortunately, after ~150 hours on stream a power cut aborted the run and the reactors were cooled down. After time on stream ~170 hours the temperatures of the reactors were increase again and the experiment was resumed. However, comparing the initial data of SGHSV = 150 000 h^{-1} with the data of the same SGHSV after 200 hours on stream a small deactivation was observed. It remains unclear if the slight deactivation was due to the power cut or the exposure to high temperature over long time, as seen in the SMR validation study.

The activities of the catalysts with higher Rh loadings are almost lumped together at SGHSV of 75 000 h^{-1}. This is due to the activity nearing equilibrium conversion and making it difficult to interpret the behaviour of the catalysts.

In Figure 5-11 the methane conversion is plotted against the Rh metal loading for the fresh catalyst after line in for SGHSV 150 000 h^{-1}. There is a clear, almost linear, increase in the activity with metal content at the lower Rh loadings. However, increasing Rh loading higher than 0.4 wt% does not appear to increase the overall activity. This can be explained that when adding more Rh, a corresponding particle size increase occurs thus not increasing the number of active sites.

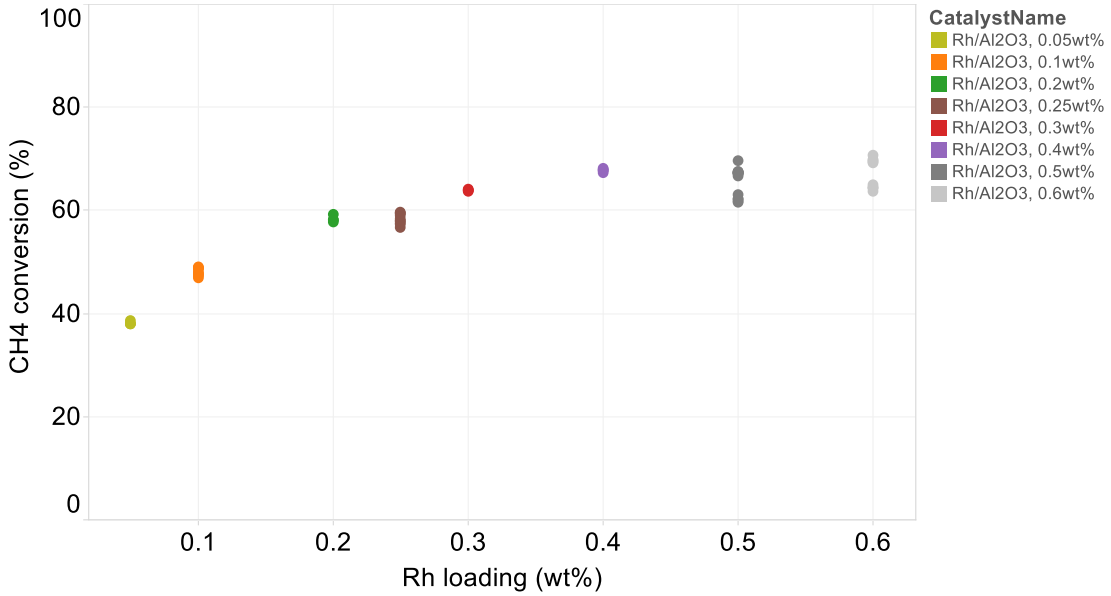

Figure 5-11: Methane conversion with various Rh loadings; GHSV = 150 000 h^{-1}, ToS = 40-80 h.

A selection of the catalysts in this study were characterised for CO chemisorption. It is assumed that the remaining catalysts follow similar trend, as the preparation and testing method was identical (the advantage of parallel experimentation). The very low metal loadings, below 0.2 wt% Rh, were too low for accurate analysis. A high increase in metal particle size was observed from 0.4 to 0.6 wt% (Figure 5-12) and is in agreement with the activity data. In Table 5-5 are the corresponding dispersions and metal surface areas.

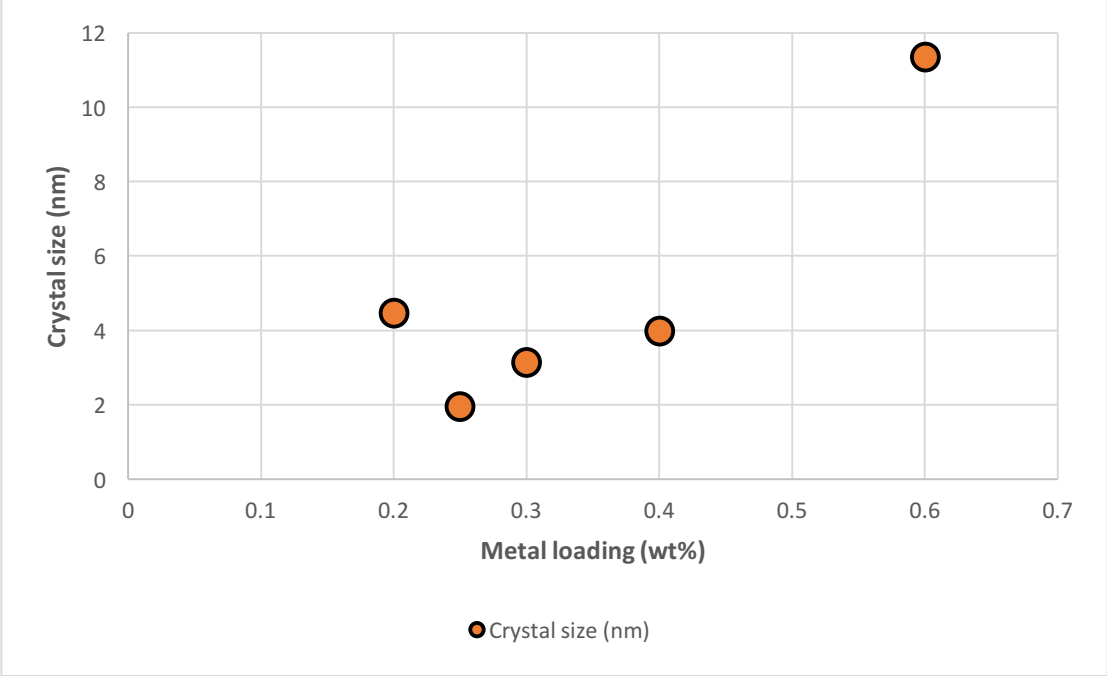

Figure 5-12: Metal particle size of Rh at different metal loadings.

Table 5-5: CO chemisorption on Rh/Al_2O_3 catalysts with varying metal loading.

Metal loading (wt%)	Metal dispersion (%)	Metal surface area (m^2/g)	Crystal size (nm)
0.2	24.5	0.22	4.5
0.25	56.3	0.62	2.0
0.3	34.9	0.46	3.1
0.4	27.5	0.48	4.0
0.6	9.7	0.26	11.3

* Nominal metal loadings are used for calculating metal dispersion, surface area and crystal size.

Figure 5-13 shows the conversion data of the catalysts at a SGHSV of 225 000 h^{-1}. A similar trend is observed where the activity increases up to a Rh loading of 0.4 wt%. This trend was detected at each space velocity, as well as after the power cut. The figures for the other conditions are included in Appendix 9.7.

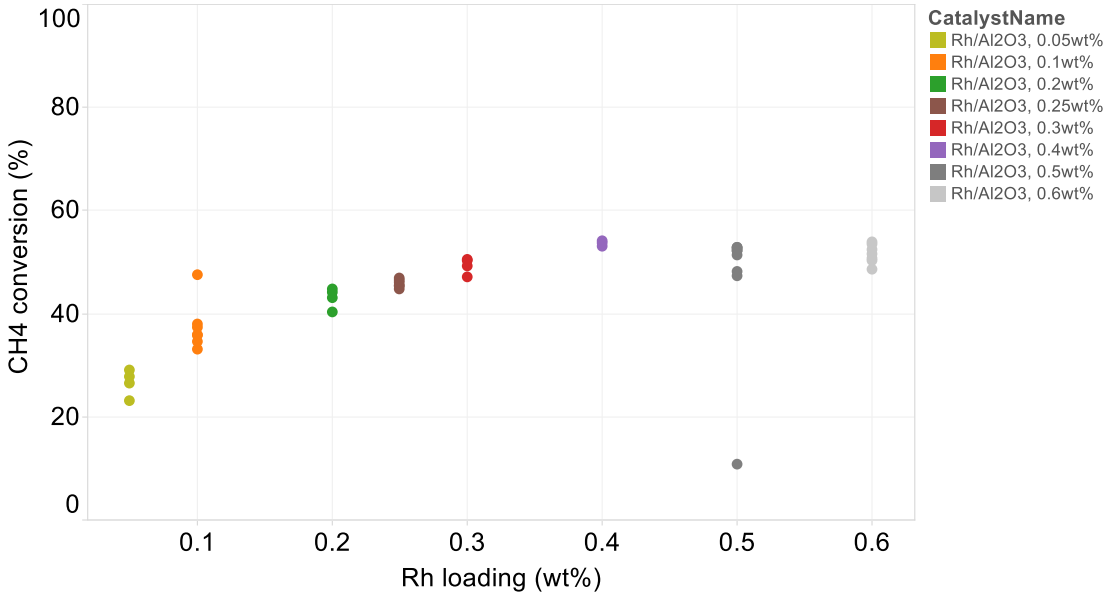

Figure 5-13: Methane conversion with different Rh metal loadings; GHSV = 225 000 h^{-1}, ToS = 120-150 h.

6 Discussion

Combinatorial chemistry and high throughput methodology (with respect to parallelisation) has been around since the early nineteen hundred's. Only since the very end of that century has high throughput equipment been developed for the chemical industry. At the turn of the century, numerous companies offered services and technology, all with the grand view of complete automation through robotics. However, due to the high costs (together with the worldwide economic recession of the early 2000's), and the complexity of research in catalysis, a full automated 'assembly-line' research has never been realised in grand scale. Nonetheless, nowadays various equipment is available for use in catalyst development and process optimisation.

Many reports are published on experiments performed in various reactors, with often variations in catalyst formulations. Unfortunately, in many cases due to time constraints it is almost impossible to proof the reproducibility of these results. Especially with manual performed experiments (e.g. catalyst preparation using conventional glassware techniques) small deviations to the procedure can have an impact on the results. The aim of this study is to demonstrate the use of high throughput equipment for the research and development of fuel processing catalysts. The first objective in the project was to present reproducible preparation of impregnation catalysts. Subsequently, the reproducibility of the testing equipment was determined through the performance for medium temperature water-gas shift and the high temperature steam methane reforming. Lastly, the third objective was to implement these techniques to determine the influence of low rhodium metal loading on its activity.

Reproducibility in catalyst preparation

Two types of catalysts were prepared by a synthesis robot for use in the reproducibility studies. A Pt/Al_2O_3 was selected for water-gas shift reaction at medium temperatures (around 300°C). Alumina supported rhodium catalyst is known to be highly active for steam methane reforming and a metal loading of 0.5 wt% was chosen for this reaction. Nine batches of a 1 wt% Pt and nine batches of 0.5 wt% Rh catalysts were prepared in parallel. All catalysts were prepared by incipient wetness impregnation.

To determine the reproducibility of the preparation the Rh series were analysed by ICP (inductively coupled plasma). Firstly, one single Rh batch was analysed in duplicate (6 times) and the metal content was determined to be 0.50 ± 3.9% (average value ± relative standard deviation as percentage of average). The ICP analysis of the Rh series (eight catalyst batches) resulted in an average measured weight loading of 0.40 ± 4.7%. The relative standard deviation (RSD) is in close agreement with the expected deviation of the ICP equipment. Nonetheless, the average metal content is slightly below the intended loading. This small deficiency in metal loading can be due to lower concentration of the metal salt stock solution. The rhodium nitrate hydrate salt is extremely hygroscopic and could have absorbed more water. Also, the rhodium content in the salt varies between batch from the supplier Sigma-Aldrich (assay ~36% Rh).

The Pt/Al_2O_3 catalyst batches were analysed for ICP as well. A metal loading of 1 wt% was aimed for and the average measured loading was 1.02 wt%. However, the RSD on these analyses was 11.8%. This is notably higher than the RSD obtained from the Rh duplicates (4.7%). The Pt series were also characterised for metal particle size by CO chemisorption and the standard deviation was calculated to be 6.8% of the average. This RSD from chemisorption is more in agreement with what

was expected and significantly lower than the RSD on ICP. Also, the deviation on the activity measurement for WGS conversion, as will be discussed below, showed a lower RDS value. It is assumed that the large deviation in the ICP analyses were attributed by the analysis technique, rather than from the catalyst preparation. One possible issue in the ICP analysis is the complete dissolution of the sample (digestion). Incomplete digestion will result in large deviations on the measured metal loading. Table 6-1 shows an overview of the characterisation results.

Table 6-1: Characterisations of Pt and Rh catalyst series.

Catalyst		**Metal loading[a] (wt%)**	**Crystal size[b] (nm)**
Pt/Al_2O_3	Average	1.02	1.67
	RSD[c]	11.8%	6.7%
Rh/Al_2O_3	Average	0.40	
	RSD[c]	4.7%	

[a] Measured by ICP,
[b] Measured by CO chemisorption,
[c] Relative standard deviation as % of average value.

WGS reproducibility

The water-gas shift (WGS) reaction was run at low temperatures (200°C) using a commercial catalyst and medium temperatures (300-350°C) with a prepared Pt/Al_2O_3 catalysts. The commercial catalyst was tested in an one-to-many study, meaning one catalyst batch tested in multiple reactors. Once the catalysts were settled in, after ~100 hours on stream, the RSD was calculated to be 6.3% of the average CO conversion of nearly 40%. It should be noted that these conversions are far below equilibrium conversions. It was shown that even after rearranging the reactors at different positions, similar activity ranking per reactor was observed. This means that a significant contribution to the standard deviation of the activity was from loading the reactor (RSD on catalyst mass per reactor = ~1%) and metal distribution of the catalyst particles.

In the many-to-many experiment, the eight prepared Pt catalyst batches were tested at various temperatures and space velocities to obtain a range of conversions. At CO conversions over 20% a RSD was calculated to be around 4%. At the low conversion of 12% the error in GC analysis increased and the RSD became 6.3% (see Table 6-2).

SMR reproducibility

For steam methane reforming a series of Rh/Al_2O_3 catalysts were prepared. In the one-to-many experiment the space velocity was increased to lower the conversions away from equilibrium. At a SGHSV of 115 000 h^{-1} the average conversion of the reactors were 73% with a RSD of less than 3%. The eight batches of 0.5 wt% Rh/Al_2O_3 were tested at the same increased space velocity and the RSD, taken at the same time on stream, was just under 4% (Table 6-2). The standard deviations from methane conversions are slightly lower than those of CO conversions due to the accuracy of the MS5 column; CO elutes after CH_4 and thus results in a slightly broader CO peak (less accurate to integrate).

Table 6-2: Comparison of RSD in activity screening.

	WGS[a]	SMR[b]
One-to-many	38.8% ± 6.3%	73.2% ± 2.7%
Many-to-many	53.2% ± 4.1%	72.5% ± 3.8%

[a] Average CO conversion ± relative standard deviation as % of average
[b] Average CH_4 conversion ± relative standard deviation as % of average

As part of the steam reforming reproducibility data was collected from various studies to assess the run-to-run reproducibility. Two catalyst batches were independently prepared by Chemspeed (on different days), as well as a same catalyst formulation prepared by hand using conventional glassware. All catalysts were prepared by IWI with a targeted metal loading of 0.5 wt% Rh. When comparing the data for methane conversions all measured activities show consistent catalyst deactivation over 400 hours on stream. Only the data from the conventional single reactor setup appeared to have lower activities. This marginally lower activity can be explained by slight differences in calibrations of MFCs and GC.

Effect of metal loading on SMR

A study of the metal loading on the activity of methane conversion in steam reforming was performed. A range of catalysts were prepared through incipient wetness impregnation on the Chemspeed platform. A similar procedure for impregnation was followed as in the reproducibility studies, only changing the rhodium salt concentration in the impregnation solutions. The catalysts were tested at three space velocities and a select few were characterised by CO chemisorption.

The three SGHSVs resulted in a wide range of conversions for all the metal loadings, although at the lower SGHSV of 75 000 h^{-1} the conversions of the high metal loadings approached equilibrium (>80% conversion). During the first 24 hours of the experiment the low Rh catalysts required time to stabilize (displayed an increasing activity over time), whereas the higher Rh loadings performed at their stable activity from start. Possibly, the smaller Rh loadings require longer reduction times then the standard activation procedure (section 4.3.6) and further reduction occurred during the reaction. By converting methane and steam to H_2 and CO, the catalysts were exposed to a reducing atmosphere.

As expected, the higher the Rh metal loading the higher the methane conversion. However, between 0.4 and 0.6 wt% Rh no significant increase was observed (Figure 5-11 and Figure 5-13). This could be explained by an increase in Rh crystal size between 0.4 and 0.6 wt% and adding more Rh only increases the crystals and not the number of active sites. This is confirmed by the CO chemisorption (Figure 5-12) that analysed a particle size for the 0.6 wt% almost 3 times that of the other catalysts (< 0.4 wt%).

7 Conclusions and recommendations

In this project two equipment were used for high throughput experimentation with the aim to validate the methodology and determine its reproducibility. The equipment was designed for research projects to develop catalysts and optimise processes for fuel processing, more specifically for steam methane reforming and water-gas shift reactions. The equipment were used for automated catalyst impregnations and parallel fixed-bed catalyst testing.

Two series of catalysts have been prepared; Pt/Al_2O_3 for WGS and Rh/Al_2O_3 for SMR reactions, as well as one commercial catalyst was used for WGS. In both reactions two type of experiments were performed to determine the standard deviation for reproducibility. The first experiments are one-to-many, where one catalyst batch (prepared or commercial) was tested in many reactors for conversion activity. The second experiments are many-to-many, in which eight batches of the same catalyst was prepared and all tested for activity.

A single 1 wt% Rh/Al_2O_3 sample was measured for 6 duplicate analyses on the ICP equipment. A standard deviation for the equipment (including the procedure) error was calculated to be 3.9%. The overview of the characterisations of the Rh and Pt catalyst series are included in Table 6-1. All RSD values are within acceptance of around 5%, except the ICP analyses of the Pt series. However, the chemisorption results are within acceptable deviation (all data within the range of the duplicate measurement). Issues with digestion of the Pt/Al_2O_3 will result in deviating results and it is suggested to reanalyse the Pt series for ICP, as well as a large duplicate sample for assessing chemisorption equipment error.

The reproducibility of the WGS and SMR reaction are assessed with both one-to-many and many-to-many experiments. The calculated RSD are represented in Table 6-2 and are all within 6%. Data for SMR, obtained in various studies on the high throughput equipment using similar catalysts, were also compared at the same condition. Figure 5-9 shows all the collected data to overlap with similar activities and slow deactivation trends. Included in this data set were catalysts prepared in conventional glassware and using the synthesis robot, as well as an experiment in a conventional single reactor setup.

A short study was performed into the effects of low Rh metal loading on the catalytic activity for steam methane reforming. A series of catalysts with Rh loadings ranging from 0.05 to 0.6 wt% were tested. A rhodium content of 0.4 wt% was observed to have the highest activity per Rh. Lower Rh content would require decreased space velocity, whereas higher metal content does not increase the conversion due to larger crystals sizes). This study has been performed up to a metal loading of 0.6 wt% and it is recommended to follow-up with studying the range of 0.6 to ~2.5 wt%.

It can be concluded that the high throughput technique, using the Chemspeed and Flowrence equipment, is reproducible with a standard deviation of ~ 4%. The high throughput methodology is incredibly efficient tool for increasing the number of experiments that can be performed within time. This enables the researcher to explore a wider (or more detailed) parameter space reaching more complete conclusions.

8 References

Acar, C. & Dincer, I. 2015. Impact assessment and efficiency evaluation of hydrogen production methods. *International journal of energy research*. 39:1757-1768. DOI:10.1002/er.3302.

Avantium, 2015. About us. Available: https://www.avantium.com/about-us/ [2016, March 10].

Chemspeed, 2015. What we do. Available: http://www.chemspeed.com/what-we-do/ [2016, March 10].

Dincer, I. & Zamfirescu, C. 2012. Sustainable hydrogen production options and the role of IAHE. *International journal of energy research*. 37:16266-16286.

Energy.gov, n.d. Office of energy efficiency & renewable energy. Available http://energy.gov/eere/fuelcells/types-fuel-cells [2016, January 3].

Ferrauto, R., Hwang, S., Shore, L., Ruettinger, W., Lampert, J., Giroux, T., Liu, Y. & Ilinich, O. 2003. New material needs for hydrocarbon fuel processing: generating hydrogen for the PEM fuel cell. *Annual review of materials research*. 33:1-27. DOI:10.1146/annurev.matsci.33.022802.091348.

Freeslate, 2016. Mission statement. Available: http://www.freeslate.com/about-freeslate/mission [2016, March 10].

Hagemeyer, A., Brooks, C., Carhart, R., Yaccato, K., Lesik, A. 2004. Methods for the preparation of catalysts for hydrogen generation. US Patent 2004/0175491 A1.

Hagemeyer, A., Carhart, R.E., Yaccato, K. Strasser, P., Herrmann, M., Grasselli, R.K., Brooks, C.J., Phillips, C.B. 2007. Catalyst formulations containing Group 11 metals for hydrogen generation. US Patent 7,179,442 B2.

hte-company, 2016. About hte. Available: http://www.hte-company.com/en/hte/about-hte [2016, March 10].

ILS, 2016. High throughput units. Available: http://www.integratedlabsolutions.com/technology-solutions/high-throughput-units/ [2016, March 10].

Joensen, F., Rostrup-Nielsen, J.R. 2002. Conversion of hydrocarbons and alcohols for fuel cells. *J. Power Sources*. 105:195-201.

Kolb, G. 2008. *Fuel processing for fuel cells*. Weinheim, Germany: WILEY-VCH Verlag GmbH & Co. KGaA.

Ligthart, D.A.J.M., Van Santen, R.A., Hensen, E.J.M. 2011. Influence of particle size on the activity and stability in steam methane reforming of supported Rh nanoparticles. *Journal of Catalysis*. 280:206-220.

Maclean, D., Baldwin, J.J., Ivanov, V.T., Kato, Y., Shaw, A., Schneider, P. 1999. Glossary of terms used in combinatorial chemistry. *International union of pure and applied chemistry*. 71:2349-2365.

Maier, W.F., Stöwe, K. & Sieg, S. 2007. Combinatorial and high-throughput material science. *Angewandte chemie international edition*. 46:6016-6067.

Morra, G., Desmartin-Chomel, A., Daniel, C., Ravon, U., Farrusseng, D., Cowan, R., Krusche, M., Mirodatos, C. 2008. High-Throughput gas phase transient reactor for catalytic material characterisation and kinetic studies. *Chemical Engineering Journal*. 138:379-388.

Potyrailo, R., Rajan, K., Stöwe, k., Takeuchi, I., Chisholm, B., Lam, H. 2011. Combinatorial and high-throughput screening of materials libraries: Review of state of the art. *ACS Combinatorial Science*. 13:579-633.

Rostrup-Nielsen, J.R. 1973. Activity of nickel catalysts for steam reforming of hydrocarbons. *Journal of Catalysis*. 31:173-199.

Rostrup-Nielsen, J.R. 1984. Catalytic steam reforming. *Catalysis Science and Technology*. Berlin, Heidelberg, Germany: Springer-Verlag.

Trimm, D.L., Önsan, Z.I. 2001. Onboard fuel conversion for hydrogen-fuel-cell-driven vehicles. *Catalysis Reviews*. 43:31-84.

U.S. Department of Energy, n.d. Energy efficiency & renewable energy. Available https://www.fueleconomy.gov/feg/fcv_PEM.shtml [2016, January 3].

Varian Micro-GC User Manual. 2005. *Galaxie Varian CP-4900 Micro-GC Control.pdf*. Available:
http://www.agilent.com/cs/library/usermanuals/public/CP501265490%20Rev1.pdf

Wang, S., Lu, G.Q. 1998. CO_2 reforming of methane on Ni catalysts: Effect of support phase and preparation technique. *Applied Catalysis B*. 16:269-277.

Appendices

9 Appendix

9.1 Chemspeed setup

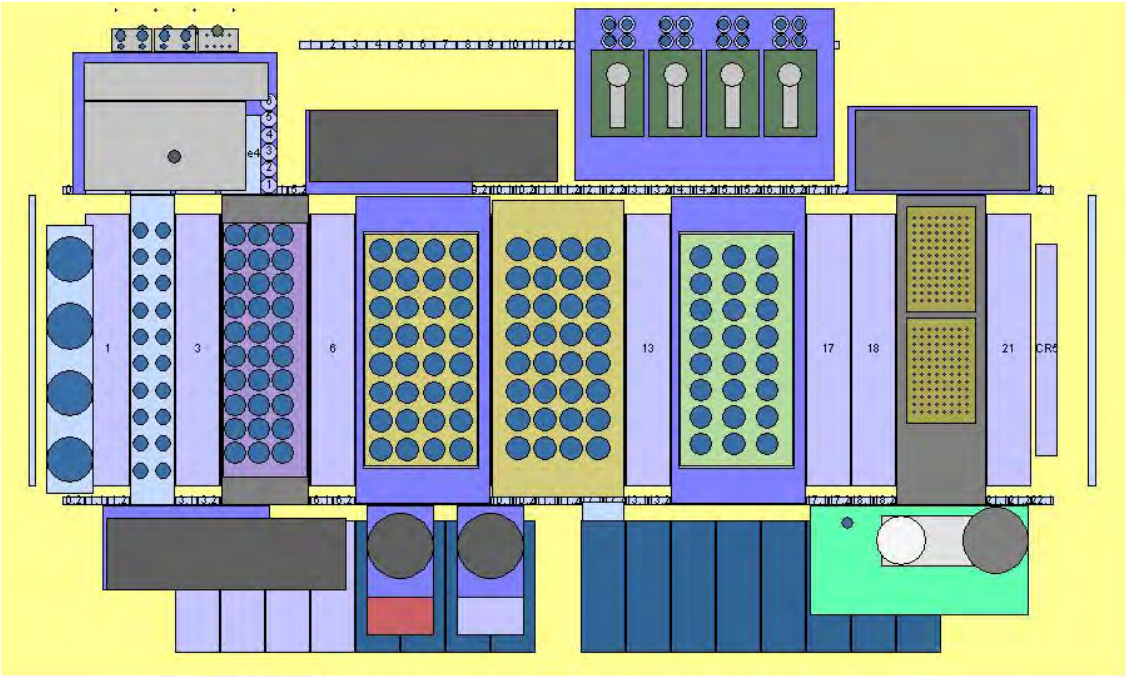

Figure 9-1: Deck layout of the Chemspeed ISYNTH platform.

9.2 Flowrence P&ID

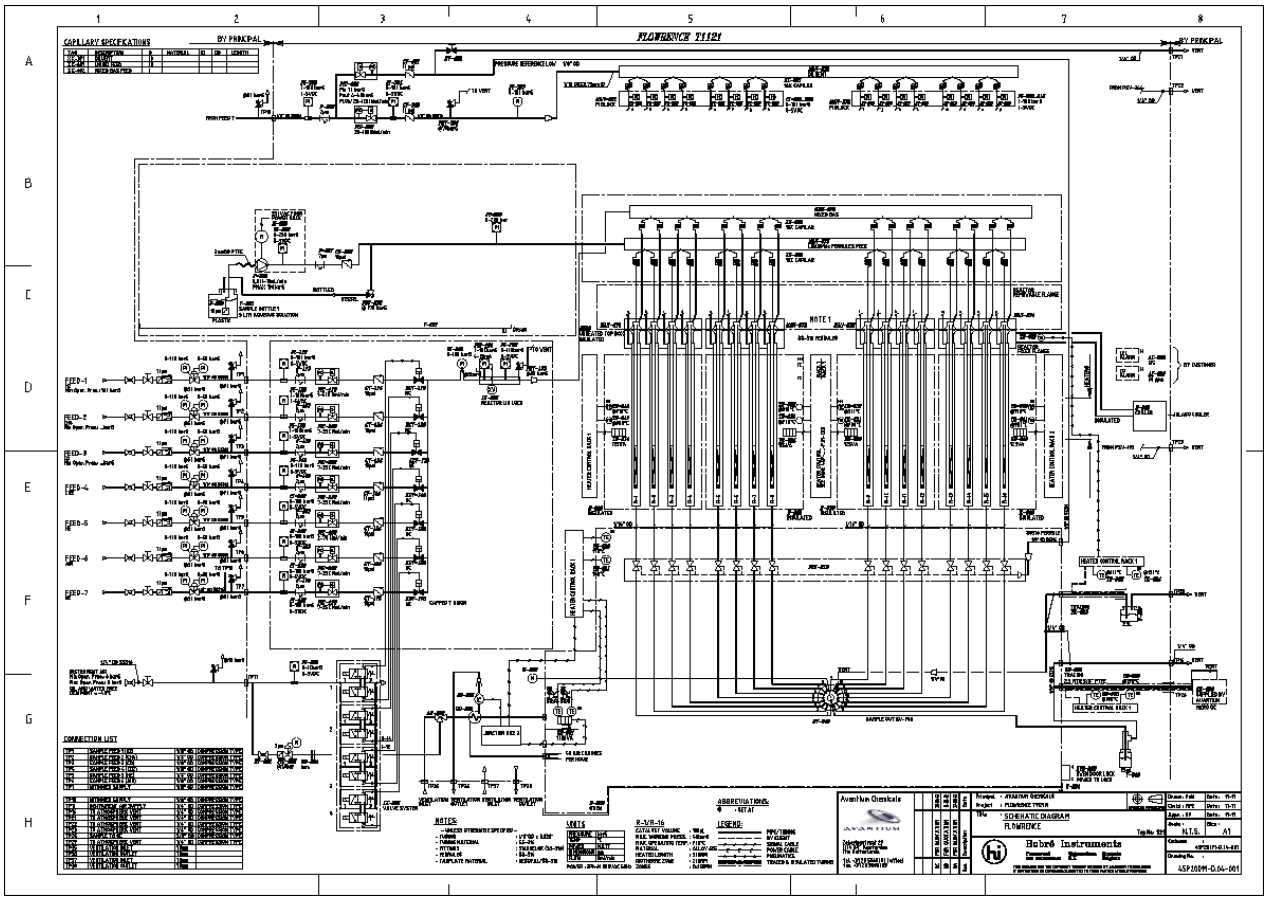

Figure 9-2: P&ID of the Flowrence parallel reactor setup.

9.3 Micro-GC analysis method

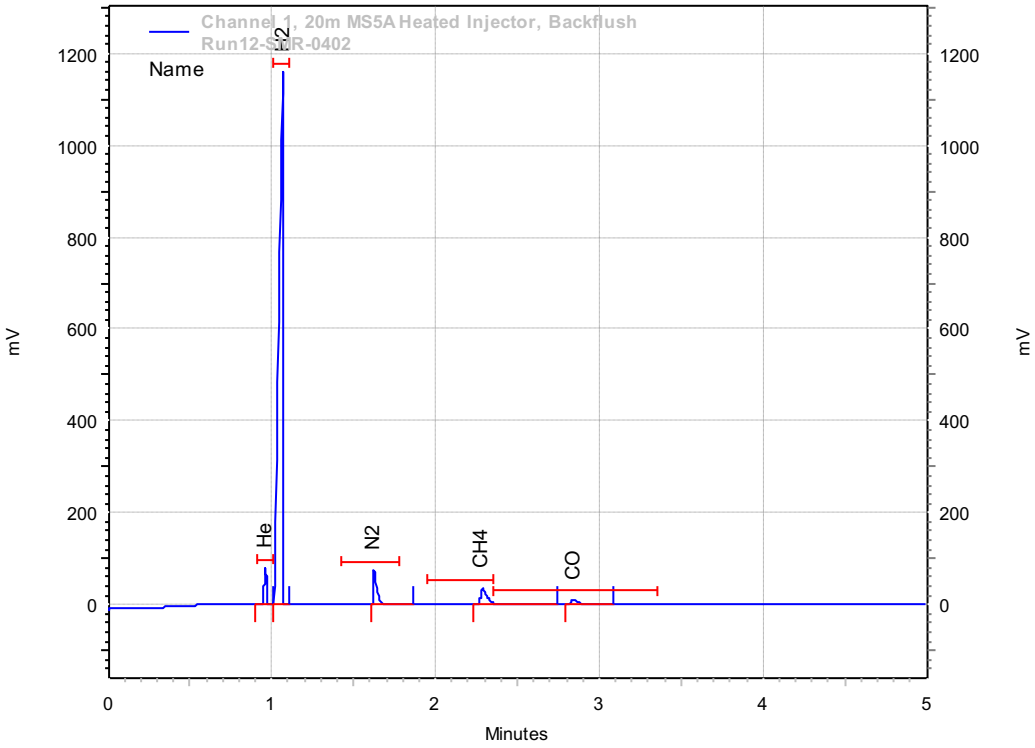

Figure 9-3: Example chromatogram from MS5 column; Catalyst 0.5 wt% Rh/Al_2O_3 (FP0067), ToS = 59.67 h, CH_4 conversion = 62.1%.

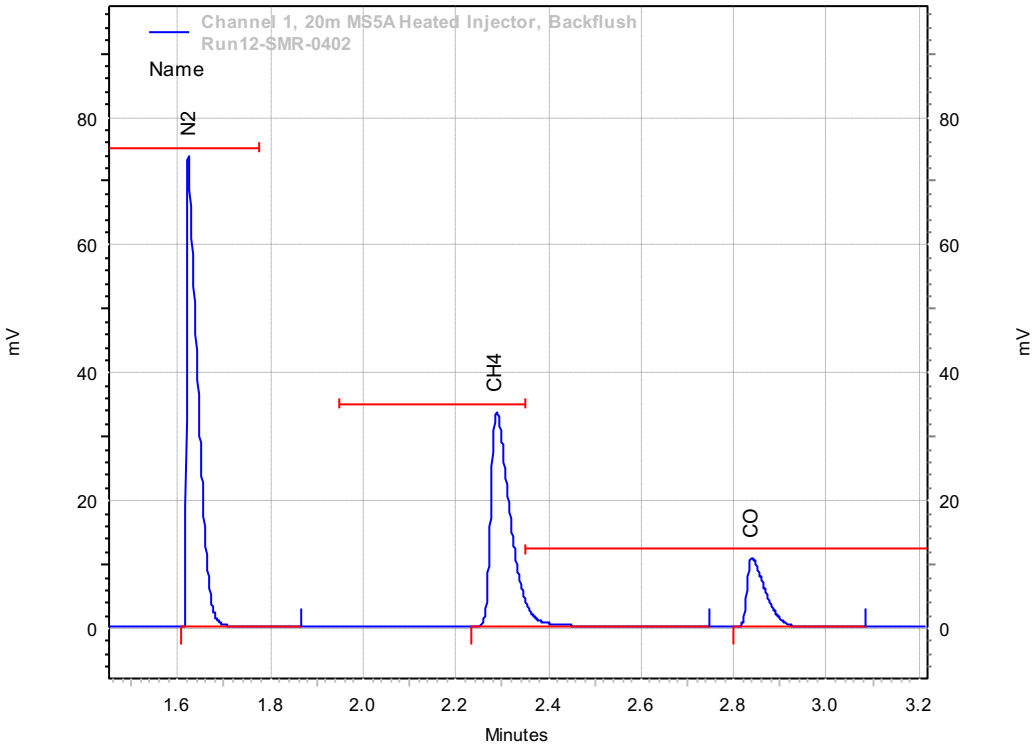

Figure 9-4: Zoomed chromatogram from MS5 column; Retention time: 1.5 - 3.2 minutes, catalyst 0.5 wt% Rh/Al_2O_3 (FP0067), ToS = 59.67 h, CH_4 conversion = 62.1%.

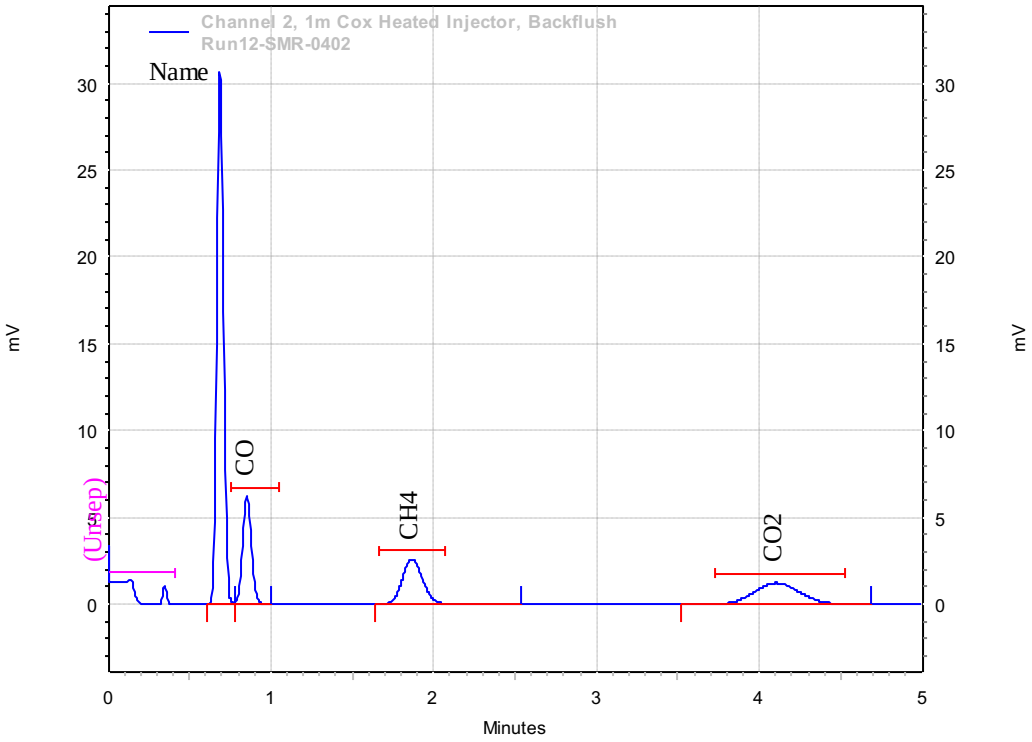

Figure 9-5: Chromatogram from COX column; Catalyst 0.5 wt% Rh/Al_2O_3 (FP0067), ToS = 59.67 h, CH_4 conversion = 62.1%.

9.4 Calibration curves

The following Figure 9-6 till Figure 9-12 and Table 9-1 and Table 9-2 are the average area count of each component in the calibration. It can be concluded that the response for all components are linear in the range operated for the experiments.

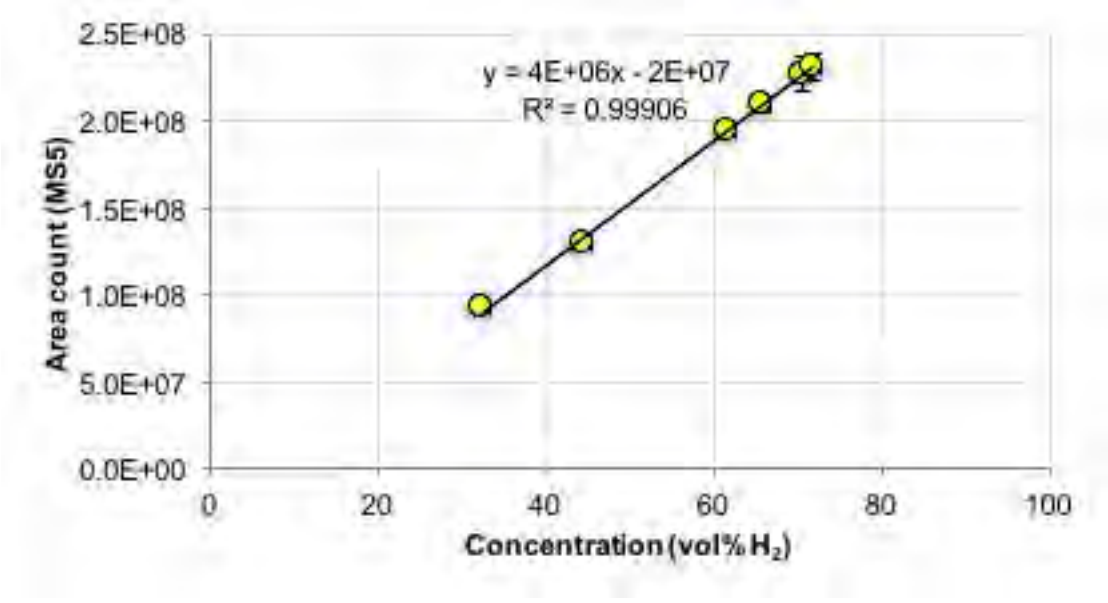

Figure 9-6: Hydrogen average response on MS5 column as concentration versus absolute area count; error bars are shown as ± standard deviation of the dataset, where no error bars are visible the error bar falls behind the data point.

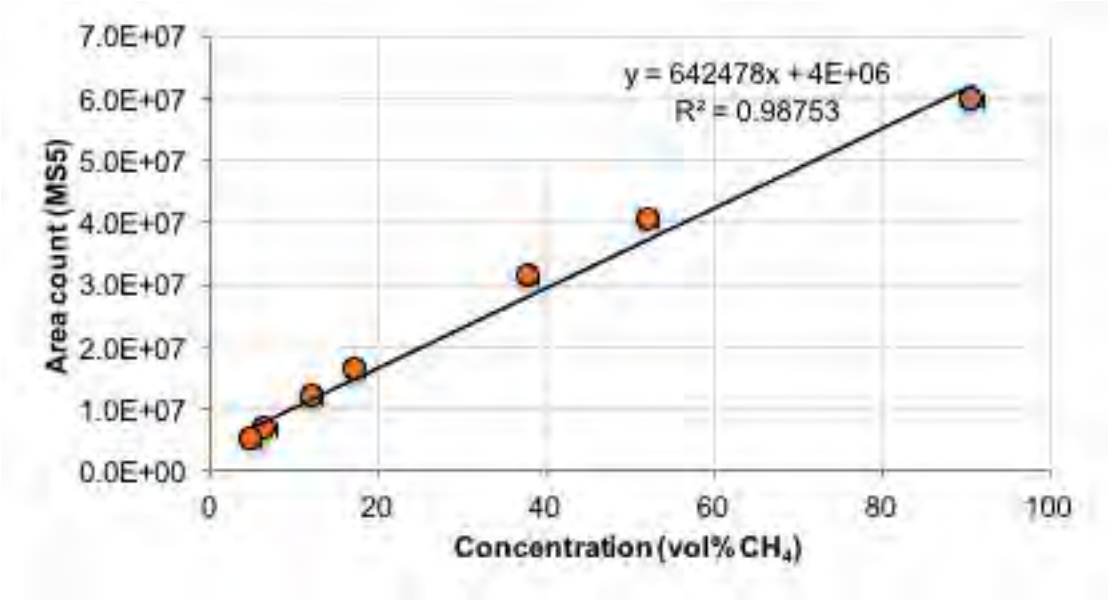

Figure 9-7: Methane average response on MS5 column as concentration versus absolute area count; error bars are shown as ± standard deviation of the dataset, where no error bars are visible the error bar falls behind the data point.

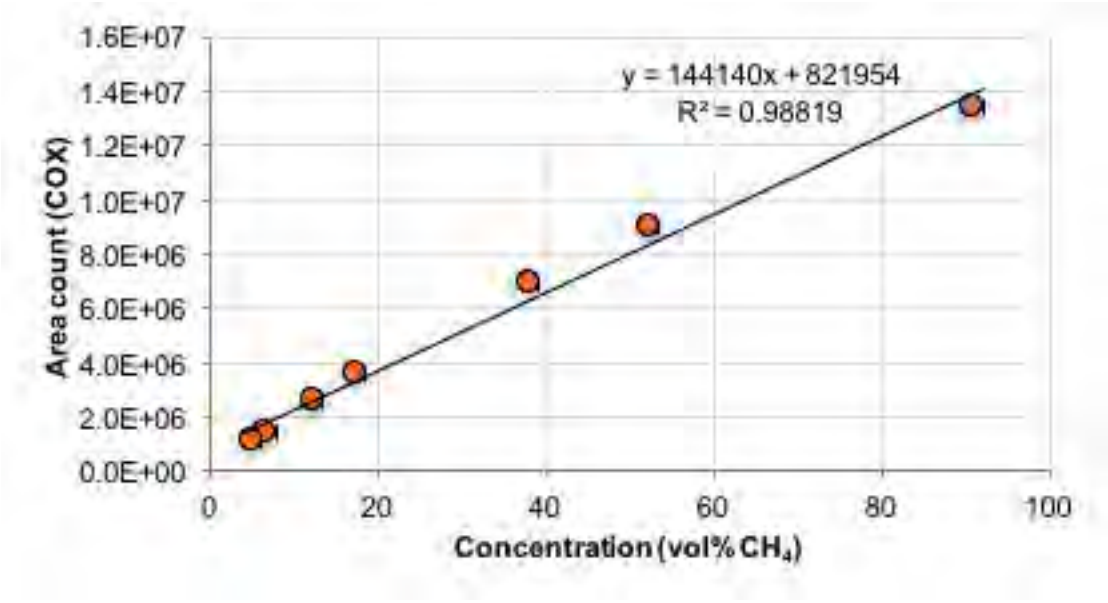

Figure 9-8: Methane average response on COX column as concentration versus absolute area count; error bars are shown as ± standard deviation of the dataset, where no error bars are visible the error bar falls behind the data point.

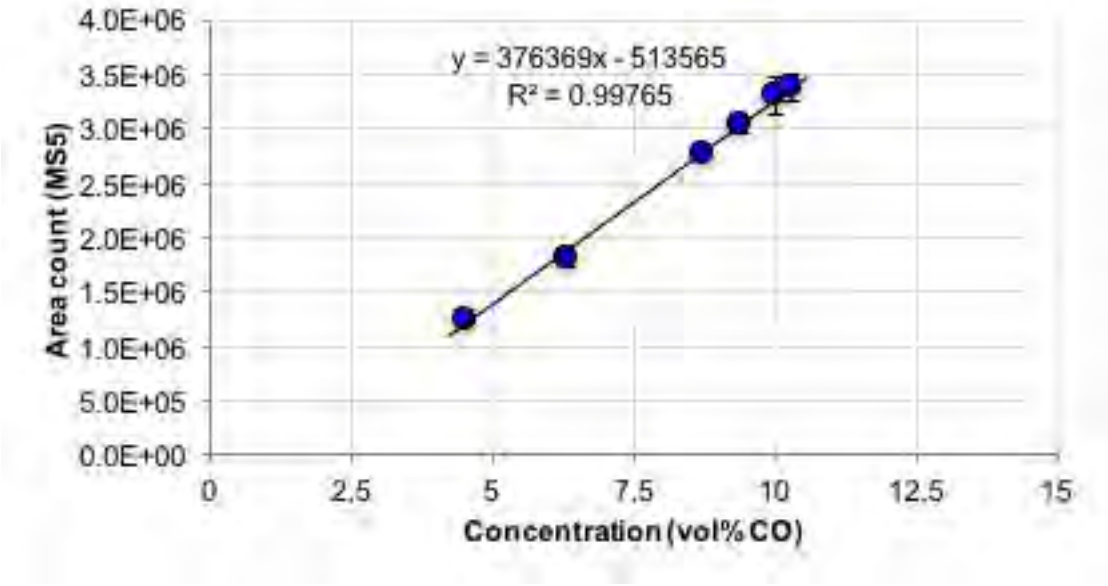

Figure 9-9: Carbon monoxide average response on MS5 column as concentration versus absolute area count; error bars are shown as ± standard deviation of the dataset, where no error bars are visible the error bar falls behind the data point.

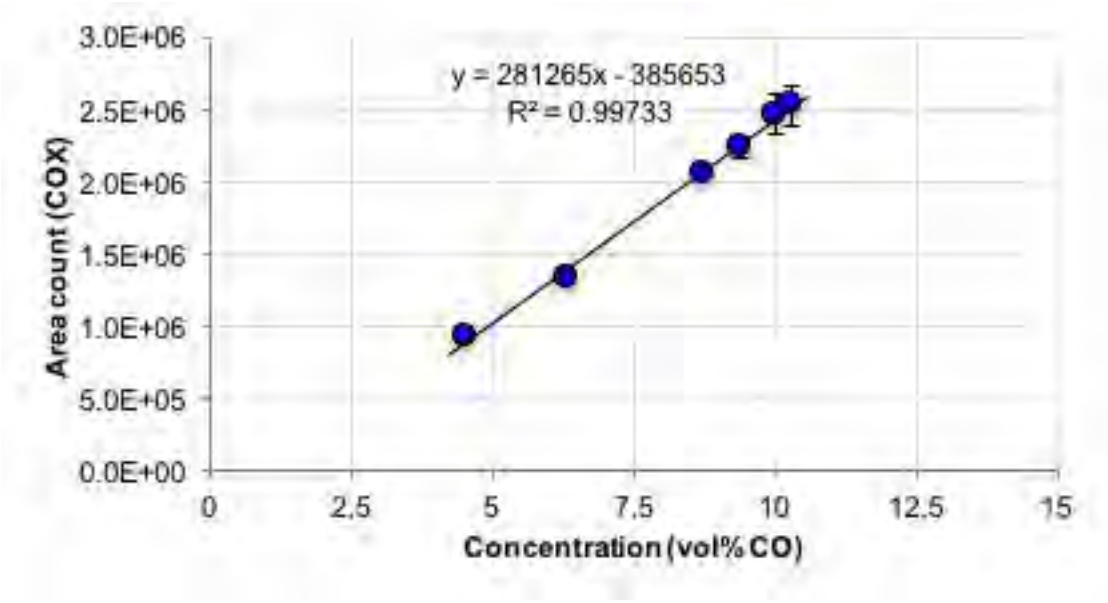

Figure 9-10: Carbon monoxide average response on COX column as concentration versus absolute area count; error bars are shown as ± standard deviation of the dataset, where no error bars are visible the error bar falls behind the data point.

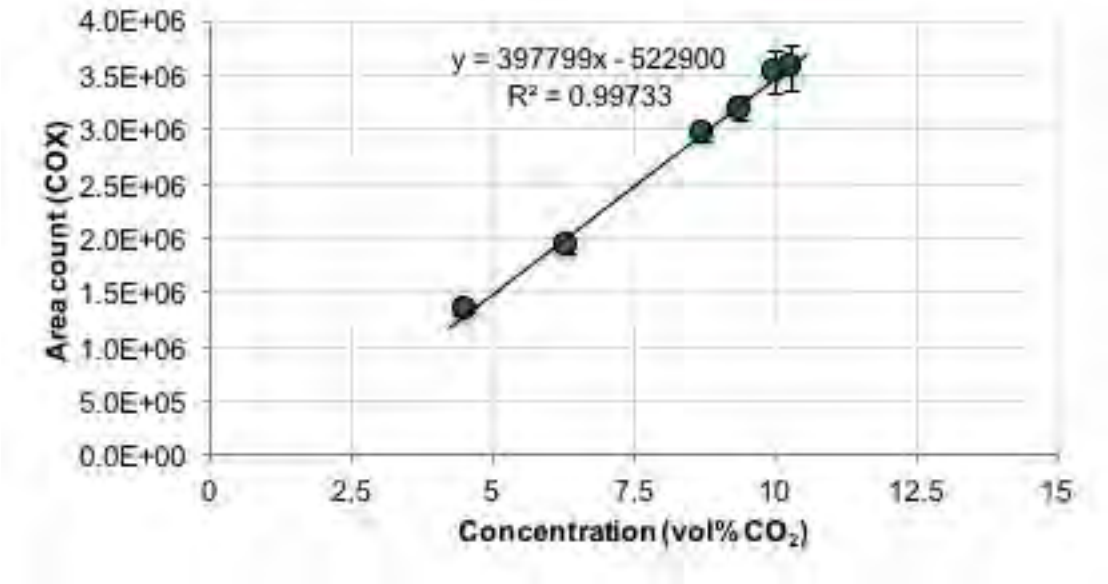

Figure 9-11: Carbon dioxide average response on COX column as concentration versus absolute area count; error bars are shown as ± standard deviation of the dataset, where no error bars are visible the error bar falls behind the data point.

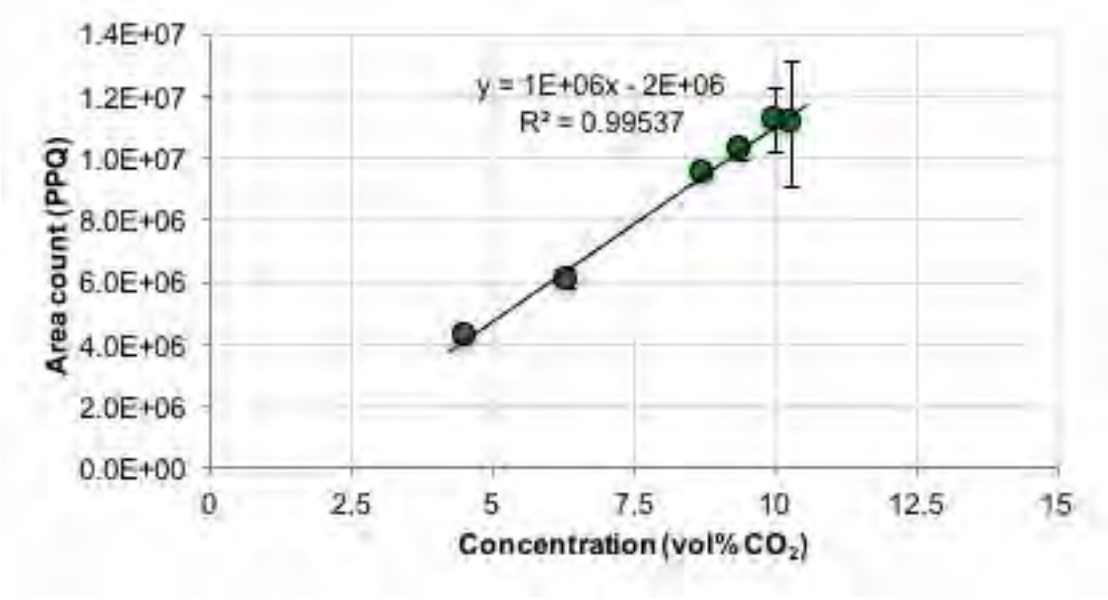

Figure 9-12: Carbon dioxide average response on PPQ column as concentration versus absolute area count; error bars are shown as ± standard deviation of the dataset, where no error bars are visible the error bar falls behind the data point.

Table 9-1: Micro-GC calibration data MS5 column; Average value of the data set ± relative standard deviation (RSD; standard deviation as percentage of average)

MS5				
He	**H2**	**CH4**	**CO**	**N2**
15686231 ± 1.4%		59554953 ± 1.2%		20217763 ± 1.2%
8510138 ± 1.3%	193601062 ± 1.2%	16108357 ± 1.4%	2763231 ± 1.3%	10882206 ± 1.3%
6806871 ± 5.1%	226798280 ± 4.6%	6403733 ± 6.8%	32893056 ± 5.2%	8854506 ± 11.6%
10908538 ± 2.8%	129778578 ± 2.8%	30974064 ± 2.9%	1790273 ± 3.0%	13971751 ± 3.0%
7762933 ± 2.4%	209128775 ± 2.2%	11694094 ± 2.4%	3019079 ± 2.4%	9906560 ± 2.4%
6496972 ± 3.5%	230564572 ± 3.1%	4911793 ± 4.7%	3365750 ± 3.6%	8258501 ± 3.6%
12528502 ± 1.4%	92309720 ± 1.3%	40173040 ± 1.4%	1241678 ± 1.5%	16032415 ± 1.4%

Table 9-2: Micro-GC calibration data COX and PPQ column; Average value of the data set ± relative standard deviation (RSD; standard deviation as percentage of average)

COX			PPQ
CH4	**CO**	**CO2**	**CO2**
13354460 ± 0.3%			
3580575 ± 1.7%	2059336 ± 1.7%	2946739 ± 1.9%	9479831 ± 1.6%
1432635 ± 7.5%	2461508 ± 5.6%	3521739 ± 5.9%	11216969 ± 9.2%
6916700 ± 3.4%	1337676 ± 3.3%	1917846 ± 3.4%	6069846 ± 4.6%
2591003 ± 3.5%	2242128 ± 3.3%	3187543 ± 3.4%	10251081 ± 2.9%
1097489 ± 6.3%	2520988 ± 5.6%	3566523 ± 5.8%	11111539 ± 18.2%
8976753 ± 0.3%	927585 ± 0.3%	1329160 ± 0.5%	4259184 ± 0.2%

9.5 Reactor loading overview

Table 9-3: Reactor loading WGS one-to-many.

Reactor position[a]	Catalyst ID	Catalyst composition	Weight (mg)
1	SM240	$CuZn/Al_2O_3$	76.8
2	Blank		
3	SM240	$CuZn/Al_2O_3$	76.1
4	SM240	$CuZn/Al_2O_3$	75.9
5	SM240	$CuZn/Al_2O_3$	76.2
6	Blank		
7	SM240	$CuZn/Al_2O_3$	77.4
8	SM240	$CuZn/Al_2O_3$	77.2
9	SM240	$CuZn/Al_2O_3$	77.6
10	SM240	$CuZn/Al_2O_3$	76.5
11	SM240	$CuZn/Al_2O_3$	76.8
12	Blank		
13	Blank		
14	SM240	$CuZn/Al_2O_3$	77.2
15	SM240	$CuZn/Al_2O_3$	77.0
16	SM240	$CuZn/Al_2O_3$	77.5
Average			***76.85***
RSD			***0.74%***

[a] Reactor position of initial start of experiment.

Table 9-4: Reactor loading WGS many-to-many.

Reactor position	Catalyst ID	Catalyst composition	Weight (mg)
1	FP0150	1 wt% Pt/Al_2O_3	149.6
2	FP0151	1 wt% Pt/Al_2O_3	150.3
3	FP0152	1 wt% Pt/Al_2O_3	149.7
4	FP0153	1 wt% Pt/Al_2O_3	149.8
5	FP0154	1 wt% Pt/Al_2O_3	150.0
6	FP0155	1 wt% Pt/Al_2O_3	150.3
7	FP0156	1 wt% Pt/Al_2O_3	149.5
8	FP0157	1 wt% Pt/Al_2O_3	150.6
9	FP0104	1 wt% Pt/Al_2O_3	149.5
10	Blank		
11	FP0151	1 wt% Pt/Al_2O_3	149.0
12	FP0155	1 wt% Pt/Al_2O_3	149.4
***Average*[a]**			***149.8***
RSD			***0.31%***
13	Blank		
14	FP0150	1 wt% Pt/Al_2O_3	75.2
15	FP0151	1 wt% Pt/Al_2O_3	74.9
16	FP0154	1 wt% Pt/Al_2O_3	75.4

[a] Average and RSD of weights of reactor 1 to 12.

Table 9-5: Reactor loading SMR one-to-many.

Reactor position	Catalyst ID	Catalyst composition	Weight (mg)
1	Blank		
2	FP0004	0.5 wt% Rh/Al_2O_3	50.7
3	FP0004	0.5 wt% Rh/Al_2O_3	50.5
4	FP0004	0.5 wt% Rh/Al_2O_3	50.9
5	FP0004	0.5 wt% Rh/Al_2O_3	50.3
6	FP0004	0.5 wt% Rh/Al_2O_3	50.6
7	FP0004	0.5 wt% Rh/Al_2O_3	50.6
8	FP0004	0.5 wt% Rh/Al_2O_3	50.5
9	FP0004	0.5 wt% Rh/Al_2O_3	50.6
10	FP0004	0.5 wt% Rh/Al_2O_3	50.3
11	Blank		
12	FP0004	0.5 wt% Rh/Al_2O_3	50.1
13	FP0004	0.5 wt% Rh/Al_2O_3	50.1
14	FP0004	0.5 wt% Rh/Al_2O_3	50.6
15	FP0004	0.5 wt% Rh/Al_2O_3	50.5
16	FP0004	0.5 wt% Rh/Al_2O_3	50.6
Average			***50.5***
RSD			***0.45%***

Table 9-6: Reactor loading SMR many-to-many.

Reactor position	Catalyst ID	Catalyst composition	Weight (mg)
1	FP0023	0.5 wt% Rh/Al_2O_3	50.5
2	FP0024	0.5 wt% Rh/Al_2O_3	50.5
3	FP0025	0.5 wt% Rh/Al_2O_3	50.5
4	FP0026	0.5 wt% Rh/Al_2O_3	50.3
5	FP0027	0.5 wt% Rh/Al_2O_3	50.5
6	FP0028	0.5 wt% Rh/Al_2O_3	50.1
7	FP0029	0.5 wt% Rh/Al_2O_3	50.5
8	FP0030	0.5 wt% Rh/Al_2O_3	50.0
9	--	--	--
10	Blank		
11	FP0024	0.5 wt% Rh/Al_2O_3	50.1
12	FP0028	0.5 wt% Rh/Al_2O_3	50.2
13	FP0004	0.5 wt% Rh/Al_2O_3	50.3
14	FP0030	0.5 wt% Rh/Al_2O_3	49.9
15	FP0030	0.5 wt% Rh/Al_2O_3	50.2
16	FP0026	0.5 wt% Rh/Al_2O_3	50.2
Average			***50.3***
RSD			***0.41%***

Table 9-7: Reactor loading SMR Rh loading.

Reactor position	Catalyst ID	Catalyst composition	Weight (mg)
1	FP0058	0.05 wt% Rh/Al_2O_3	24.9
2	FP0059	0.1 wt% Rh/Al_2O_3	25.1
3	FP0063	0.3 wt% Rh/Al_2O_3	24.8
4	FP0061	0.2 wt% Rh/Al_2O_3	25.1
5	Blank		
6	FP0069	0.6 wt% Rh/Al_2O_3	24.9
7	FP0062	0.25 wt% Rh/Al_2O_3	25.1
8	FP0065	0.4 wt% Rh/Al_2O_3	25.1
9	Blank		
10	FP0067	0.5 wt% Rh/Al_2O_3	25.1
11	FP0059	0.1 wt% Rh/Al_2O_3	25.3
12	FP0069	0.6 wt% Rh/Al_2O_3	25.1
13	FP0028	0.5 wt% Rh/Al_2O_3	25.2
14	FP0067	0.5 wt% Rh/Al_2O_3	25.4
15	FP0028	0.5 wt% Rh/Al_2O_3	25.4
16	FP0062	0.25 wt% Rh/Al_2O_3	25.0
Average			***25.06***
RSD			***0.55%***

9.6 Experimental results

Due to the large amount of data collected in the experiments, the raw data and calculated results are available on request.

9.7 SMR activities with metal loading increases

Below are additional figures showing similar trends as Figure 5-11 at different GHSV (*Figure B 1*, *Figure B 2*, *Figure B 3*, *Figure B 4*).

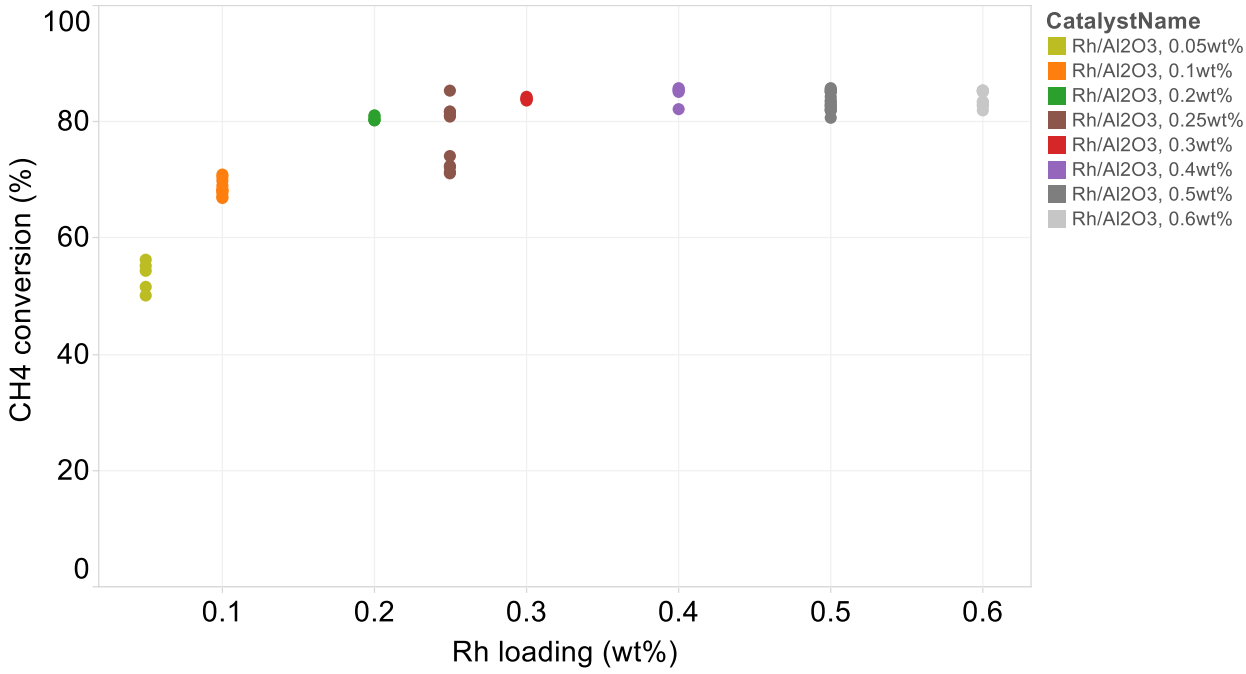

Figure B 1: Methane conversion with various Rh loadings; GHSV = 75 000 h^{-1}.

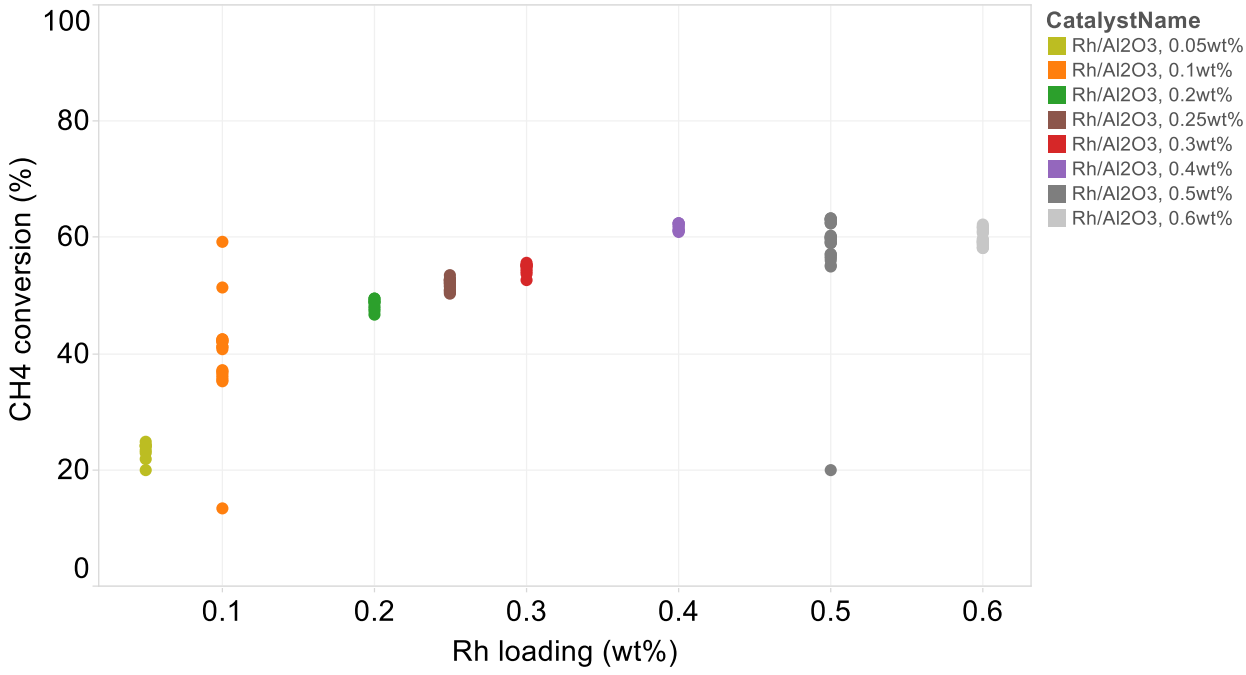

Figure B 2: Methane conversion with various Rh loadings; GHSV = 150 000 h^{-1}, ToS = 195-270 h.

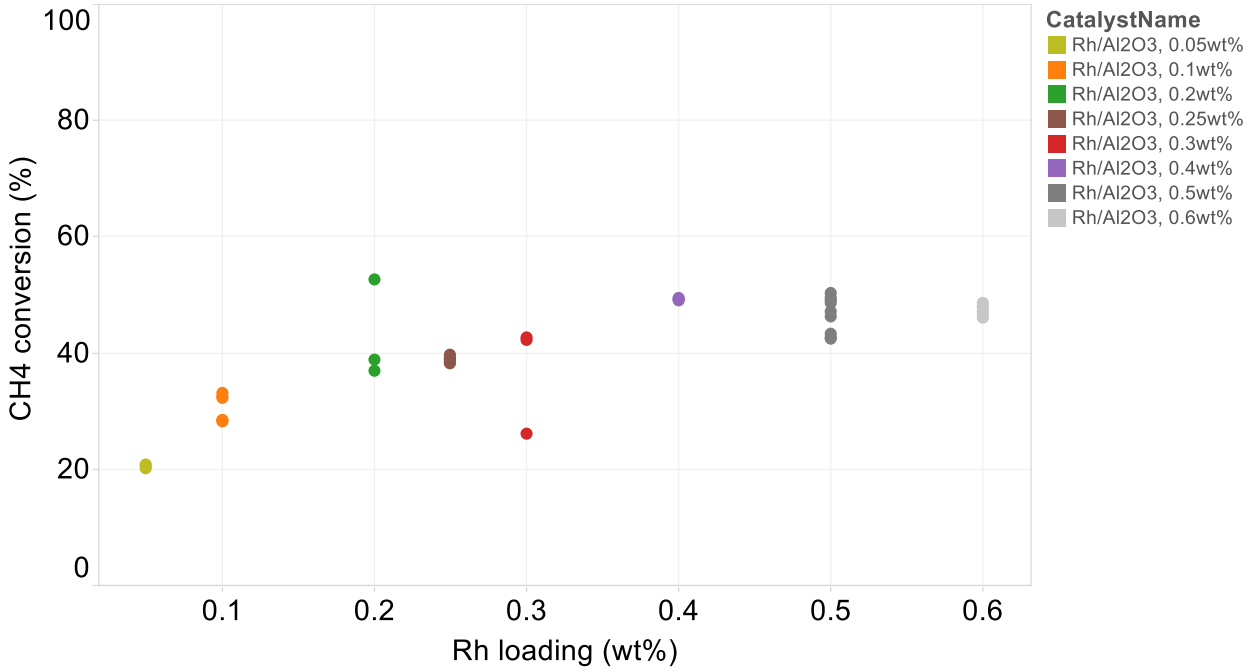

Figure B 3: Methane conversion with various Rh loadings; GHSV = 225 000 h^{-1}, ToS = 170-195 h.

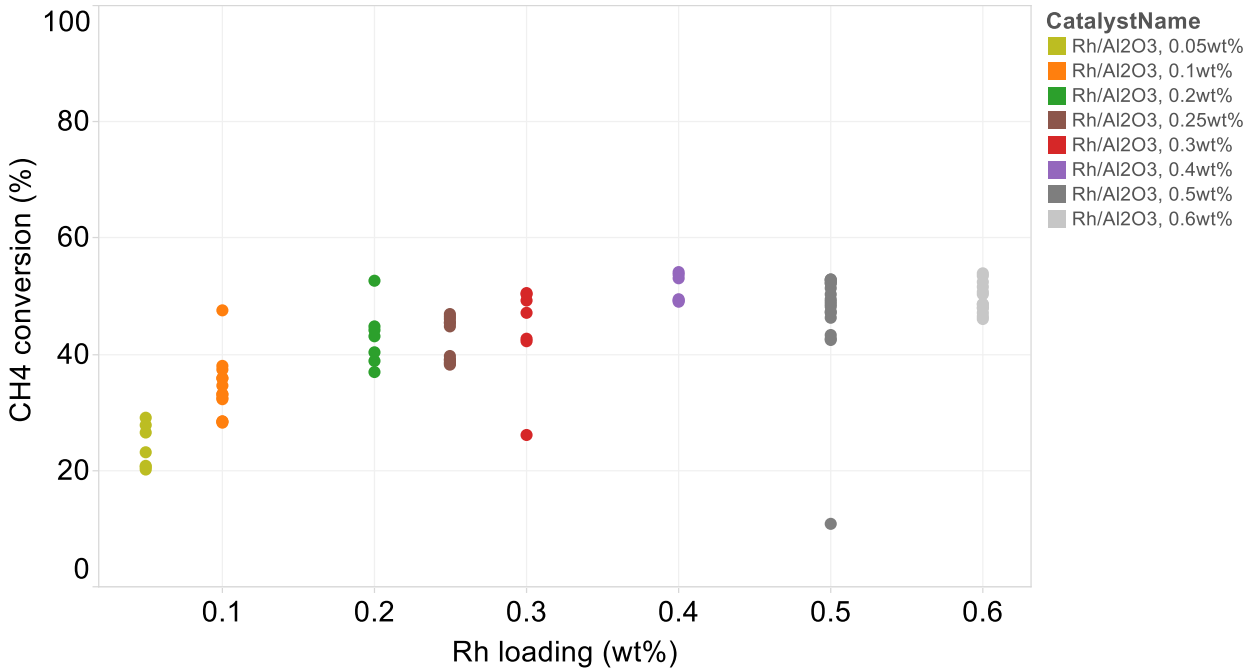

Figure B 4: Methane conversion with various Rh loadings; GHSV = 225 000 h^{-1}, ToS = 120-195 h.